


Review

# Multi-Template Molecularly Imprinted Polymeric Electrochemical Biosensors

Meltem Agar<sup>1,2</sup>, Maisem Laabei<sup>3,4</sup>, Hannah S. Leese<sup>1,5</sup> and Pedro Estrela<sup>1,2,\*</sup> 

<sup>1</sup> Centre for Bioengineering & Biomedical Technologies (CBio), University of Bath, Bath BA2 7AY, UK; ma2680@bath.ac.uk (M.A.); hsl25@bath.ac.uk (H.S.L.)

<sup>2</sup> Department of Electronic and Electrical Engineering, University of Bath, Bath BA2 7AY, UK

<sup>3</sup> Department of Life Sciences, University of Bath, Bath BA2 7AY, UK; maisem.laabei@bristol.ac.uk

<sup>4</sup> School of Cellular and Molecular Medicine, University of Bristol, Bristol BS8 1TD, UK

<sup>5</sup> Department of Chemical Engineering, University of Bath, Bath BA2 7AY, UK

\* Correspondence: p.estrela@bath.ac.uk

**Abstract:** Dual- or multi-template molecularly imprinted polymers have been an attractive research field for many years as they allow simultaneous detection of more than one target with high selectivity and sensitivity by creating template-specific recognition sites for multiple targets on the same functional monomer. Dual/multi-template molecular imprinting techniques have been applied to identify, extract, and detect many targets, from heavy metal ions to viruses, by different methods, such as high-performance liquid chromatography (HPLC), liquid chromatography–mass spectrometry (LC-MS), and piezoelectric, optical, and electrochemical methods. This article focuses on electrochemical sensors based on dual/multi-template molecularly imprinted polymers detecting a wide range of targets by electrochemical methods. Furthermore, this work highlights the use of these sensors for point-of-care applications, their commercialization and their integration with microfluidic systems.

**Keywords:** molecularly imprinted polymer; multi-template; electrochemical sensor



Received: 14 November 2024

Revised: 16 December 2024

Accepted: 1 January 2025

Published: 8 January 2025

**Citation:** Agar, M.; Laabei, M.; Leese, H.S.; Estrela, P. Multi-Template Molecularly Imprinted Polymeric Electrochemical Biosensors.

*Chemosensors* **2025**, *13*, 11. <https://doi.org/10.3390/chemosensors13010011>

**Copyright:** © 2025 by the authors. Licensee MDPI, Basel, Switzerland. This article is an open access article distributed under the terms and conditions of the Creative Commons Attribution (CC BY) license (<https://creativecommons.org/licenses/by/4.0/>).

## 1. Introduction

There is a pressing worldwide need to detect a wide range of substances that affect human health, food safety, water quality and the environment; for example, human biomarkers, drugs, bacteria, heavy metal ions, pesticides, etc. [1–5]. The detection method, therefore, should be cheap, rapid, reliable, have high selectivity and specificity and not require intense people-power. In simplistic terms, biosensors are analytical devices consisting of a transducer and a bioreceptor (target recognition molecule). Ideally, they are easy to use, fast responding, have high selectivity toward the target and do not require sample preparation beforehand. Molecules such as antibodies, aptamers, peptides, deoxyribonucleic acids and enzymes are used as bioreceptors in biosensors [6]. Although the combination of natural receptors with label-free transducers allows for the successful implementation of a plethora of sensor devices, natural biological receptors also have inherent drawbacks: their chemical and physical stability and shelf-life are limited, especially antibodies and enzymes. Additionally, their compatibility with most transducer surfaces is limited, necessitating the design of adequate linker layers.

Some of the disadvantages of natural receptors can be overcome by employing so-called antibody mimetics: robust, artificial receptors that are able to bind their targets with an affinity comparable to their natural counterparts. Molecularly imprinted polymers

(MIPs) have great potential to be robust artificial receptors. The history of molecular imprinting dates back to the 1930s, when Polyakov synthesized silica gel in the presence of aromatic hydrocarbons. By the 1970s, researchers began using different templates for imprinting silica gel. In 1970 and 1972, organic polymers replaced silica gels, and non-covalent imprinting was introduced by Mosbach, marking significant advancements in the field [7,8].

MIPs offer high specificity, stability, cost-effectiveness, and reusability, while also being budget-friendly, simple to utilize, highly selective, and sensitive to targets. On the other hand, they have limitations such as template leakage, slow binding kinetics, cross-reactivity and lower affinity.

The synthesis of MIPs is straightforward and consists of three steps: (i) formation of the functional monomer and template; (ii) polymerization of the functional monomer–template complex with the cross-linker and initiator; and (iii) template removal to create three-dimensional cavities for specific recognition [9].

The interaction between a template and functional monomers that takes place in the first stage of MIP synthesis is crucial as it affects the physical properties and recognition of the MIP and the stability of the template–monomer complex [10]. Among these interactions, non-covalent interaction is the most preferred. In this approach, the template–monomer complex interacts via van der Waals forces, hydrogen bonding,  $\pi$ – $\pi$ , dipole–dipole or ion–dipole interactions. They are weak interactions and offer some advantages, such as easy binding and template removal from the polymer, permitting a simplified process that eliminates the requirement for chemical derivatization of the template [7].

MIPs are commonly formed via free radical polymerization, which includes bulk, multi-step swelling, suspension, emulsion, seed, and precipitation polymerization. These polymerization methods suffer from low imprinting capacity, the need for a large amount of template, poor recognition and incomplete template removal [11]. In order to eliminate or ease these drawbacks, different MIP preparation techniques, such as the sol-gel process, surface and epitope imprinting and electropolymerization, have been adopted [12–14]. It is important to choose the most suitable polymerization technique according to the chemical and intrinsic properties of the template. For example, the sol-gel method allows MIP fabrication at room temperature and prevents thermal decomposition of the template, but at the same time, there is a risk of the template dissolving in the solvent. Likewise, while surface imprinting allows for high binding capacity, it requires the use of pure templates. The dimensions of the template are also important in determining the polymerization method to be chosen: polymerization methods used for small molecules might not be suitable for macromolecules such as bacteria and cells. If an appropriate method is not found, the template molecules might not be effectively removed from the polymer matrix or might not be properly imprinted.

These are very important parameters that affect the performance of the MIP. For example, functional monomers strongly interact with the target via functional groups of the target to form a template–functional monomer complex. If a suitable monomer is not chosen, a stable template–monomer complex cannot be achieved, leading to unsuccessful molecular recognition. In order to arrange the configuration of a functional monomer around the template to obtain a rigid polymeric matrix, cross-linkers are used. The amount of cross-linker has an influence on the mechanical stability of the polymeric matrix and recognition sites. The porogen and initiator are responsible for forming a porous structure, which enables the template to diffuse through an MIP and start polymerization thermally or photochemically [11,15].

MIPs allow multiplexed detection as long as they are imprinted with multi-targets (templates) under appropriate conditions. With multi-target MIPs (MT-MIPs), which are

imprinted with more than one target, simultaneous detection of at least two targets can be achieved using less material, reducing the costs and time requirements. The MT-MIP preparation steps and different interactions between the templates and the functional monomer are shown in Figure 1. The preparation of MT-MIPs is similar to that of MIPs imprinted with a single template. The synthesis of MT-MIPs begins with the formation of complexes between the different templates and functional monomers through covalent or non-covalent interactions. This is followed by the simultaneous polymerization of the functional monomer–template complexes with a cross-linker and an initiator. In the final step, the templates are removed from the polymer to create three-dimensional cavities for specific recognition [16]. Various types of interactions are employed in the fabrication of MT-MIPs, as shown in Figure 1. Different polymerization methods, such as bulk polymerization, precipitation polymerization, emulsion polymerization, suspension polymerization, electropolymerization, and surface imprinting polymerization, can be used to fabricate MT-MIPs. As per single-template MIPs, each polymerization method has its own drawbacks and should be selected based on the properties of the templates.

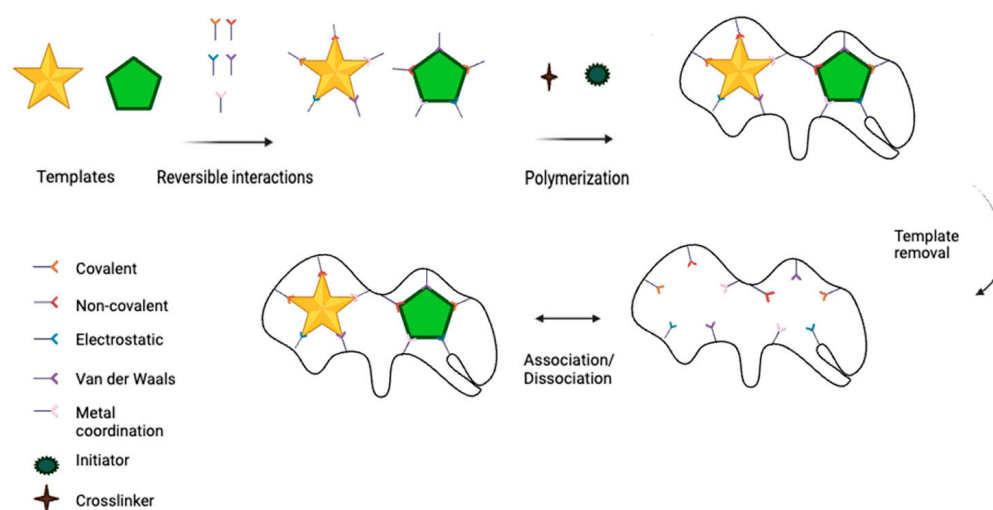


**Figure 1.** Preparation procedures for MT-MIPs and various interactions of templates (analyte) and MT-MIPs.

Since non-covalent interactions are advantageous—they allow for easier template removal, the creation of reusable recognition sites, and dynamic interactions—monomers that can form non-covalent bonds with templates are preferred. Examples include methacrylic acid (MAA) [17], acrylamide (AM) [18], 4-vinylpyridine (4-VP) [19], and 2-vinylpyridine (2-VP) [20]. The choice of cross-linker should take into account the interaction between the templates and the monomers; an inappropriate cross-linker can disrupt or break the bonds between them. For this reason, divinylbenzene (DVB) [21] and ethylene glycol dimethacrylate (EGDMA) [22] are generally used to support non-covalent interactions. For instance, Nurrokhimah et al. synthesized a molecularly imprinted polymer incorporated with graphene oxide and magnetite nanoparticles, which was used as a magnetic solid-phase extraction adsorbent for the simultaneous extraction and determination of cefoperazone, cephalexin, and cefazolin [23]. For the synthesis of MT-MIPs,  $\text{Fe}_3\text{O}_4@\text{SiO}_2\text{-NH}_2/\text{GOx}$  nanoparticles were first dispersed in acetonitrile with a specific amount of cefoperazone, cefazolin, and cephalexin as templates. The functional monomer MAA was added, and the mixture was sonicated for 15 min and then stirred for 12 h at room temperature. The solution was transferred to a three-neck flask, and EGDMA and AIBN were added as the cross-linker and initiator, respectively. Polymerization occurred under a nitrogen atmosphere at 60 °C for 24 h. Subsequently, the coated nanoparticles were

washed with a mixture of methanol and acetic acid (8:2, *v/v*) to remove the template molecules, followed by a methanol rinse. The final nanocomposite adsorbent was dried under a vacuum. In this study, MAA was chosen as the functional monomer due to its carboxyl group, which can form strong hydrogen bonds and ionic interactions with the templates. EGDMA was used as the cross-linker because of its ability to create a rigid polymer network. EGDMA is ideal for ensuring that the polymer matrix remains stable and maintains its shape even after template removal and reusability, and it does not disrupt the hydrogen bonds between MAA and the templates. The bulk polymerization technique was used for polymer formation with this method, where AIBN (azobisisobutyronitrile) was employed as the initiator to start the polymerization process. A porogen (solvent mixture), typically acetonitrile, was used to help dissolve the monomer and ensure the formation of a uniform polymer matrix. The choice of these chemicals, coupled with the bulk polymerization method, provided an effective strategy for creating highly selective and reusable MT-MIPs for pharmaceutical applications.

While preparing MIPs, there are points to be taken into consideration regardless of whether it is a multi- or single-target MIP, including the selection and amount of monomer, cross-linker, porogen and initiator suitable for the target, the use of an appropriate polymerization method and the choice of effective washing solution [10,24]. Choosing templates with the same features is important in terms of the easy preparation of MT-MIPs and the templates showing the same interactions with other MIP components. If templates with different properties are selected, MT-MIPs are more difficult to prepare, and one target may not be imprinted as effectively as the other or may not be removed from the polymer matrix after washing. Therefore, while preparing MT-MIP with templates with different features, the properties of the different types of templates to be imprinted should be considered separately and the appropriate polymerization method and MIP components should be selected accordingly. In this context, templates used in molecular imprinting can be divided into four groups: ions, organic molecules, biomacromolecules and cells/viruses [25].

Similar to MIPs, imprinting three-dimensional biomolecules in MT-MIPs poses challenges due to their high molecular weights and sizes, particularly regarding template removal and low binding efficiency. To overcome these challenges, alternative imprinting strategies such as surface imprinting and epitope imprinting have been developed. Surface imprinting creates recognition sites at or near the surface of the MIP, allowing biomolecules to access the cavities more easily. This improves the binding efficiency and facilitates efficient template removal. On the other hand, epitope imprinting uses an epitope—a small, recognizable fragment or sequence of the biomolecule—as the template instead of the entire molecule. This strategy simplifies template removal and reduces the risk of incomplete elution or cavity deformation, further enhancing the efficiency and precision of the imprinting process [26,27].

The fact that MT-MIPs allow for the simultaneous detection of multiple templates is a significant advantage over MIPs; however, the detection performance of MT-MIPs also needs to be evaluated. In several studies, MT-MIPs demonstrated similar results when detecting templates both individually and as mixtures, maintaining consistent linear ranges and limits of detection (LODs) [28–30]. For instance, in the study conducted by Fatma et al., the MT-MIP for chlorambutil and dacarbazine achieved LODs of 0.037 ng/mL and 0.016 ng/mL in mixtures, and 0.035 ng/mL and 0.014 ng/mL individually [28]. In comparison, the LOD for dacarbazine obtained with the MIP developed by Prasad et al. was 0.02 ng/mL [31]. These results demonstrate that if the appropriate MIP components and methods are selected, MT-MIPs can detect templates with high selectivity and sensitivity.

Several techniques, such as fluorescence [32–34], quartz crystal microbalance (QCM) [35,36], chemiluminescence [37,38], high-performance liquid chromatography

(HPLC) [39], surface-enhanced Raman scattering (SERS) [40] and electrochemical methods [41,42], have been used in relation to MT-MIPs. Among them, electrochemical methods are regarded as a more efficient technique in terms of the detection of many different targets since these methods have advantages in their simple manipulation, cost-effectiveness, high sensitivity, easy sample preparation steps, simplicity and fast response [43,44]. In the same study conducted by Fatma et al., the performance of the electrochemical MT-MIP was compared with HPLC and UV methods, revealing that the limit of detection achieved with the electrochemical methods was significantly lower than that obtained with HPLC and UV [28]. This underscores the sensitivity of electrochemical methods compared to other detection techniques.

To date, MT-MIPs have been used to detect many different targets simultaneously. In this review, the detection of a variety of targets by electrochemical methods will be discussed according to their target classification. The performance of MT-MIPs in aqueous solutions will be evaluated. Recent progress in MT-MIP-based electrochemical sensors for point-of-care applications will be reviewed and their commercialization and integration with microfluidic systems will be assessed.

## 2. Detection of Targets by MT-MIP

### 2.1. Detection of Ions

Many different targets can be detected by molecularly imprinted polymer-based sensors and one of these targets is ions. Imprinted polymers prepared for the detection of ions can be called “ion-imprinted polymers” instead of molecularly imprinted polymers. While the target for molecularly imprinted polymers is molecules, for an ion-imprinted polymer, it is an ion [45]. Ion-imprinted polymers are attractive as they have high environmental stability, reusability and easy synthesis processes [46].

Some elements are essential for our health and nutrition and the proper function of our immune system, such as zinc and copper; however, their excessive intake can be harmful. On the other hand, certain elements, such as heavy metals and lanthanides, are extremely toxic at minute concentrations and if ingested or exposed to can cause serious health problems. Accordingly, detection of these elements is vital and they need to be detected in a highly sensitive and selective manner.

Prasad et al. demonstrated an electrochemical sensor to detect cadmium and copper, aiming to prevent the side effects of excessive exposure to or intake of these heavy metal contaminants. The sensor was fabricated using a biocompatible monomer (2-acrylamidoethyl dihydrogen phosphate (AEDP)), a trapped ligand (L-histidine), a cross-linker (ethylene glycol dimethacrylate (EGDMA)) and an initiator (2,2-azoisobutyronitrile (AIBN)) that were thermo-polymerized with template ions and embedded in a sol-gel matrix [47]. The inter-metallic effect between Cd(II) and Cu(II) was reduced by cavities created after ion removal because cavities allow strong and independent binding. Reducing the inter-metallic effect also significantly reduced the non-linear relationship between the peak current and ionic concentration. The recognition capability of the dual-ion-imprinted polymer was assessed by differential pulse anodic stripping voltammetry (DPASV). The sensor exhibited a limit of detection (LOD) of 0.053 and 0.035 ng/mL for Cd(II) and Cu(II) ions, respectively. The limit of detection for Cd(II) of the sensor produced is lower than the safe drinking water limit (3 µg/L) determined by the World Health Organization [48]. In addition, the produced sensor exhibited a lower LOD in terms of detecting Cu than previously reported Cu MIP sensors [49,50].

In another study by Prasad et al., screen-printed carbon electrodes (SPCE) were modified with COCl-modified magnetic iron oxide nanoparticles (NPs) by drop casting (Figure 2) [51]. Thermal polymerization with the functional monomer (but-2-enedioic acid



bis-(2-amino-ethyl)-amide]] was employed in the presence of template ions (cerium(IV) and gadolinium(III)), cross-linker, initiator and multiwalled carbon nanotubes (MWCNTs). HCl solution was used to remove ions from the polymeric matrix to create cavities. After simultaneous analysis of Ce(IV) and Gd(III) by DPASV, the LOD was obtained as 0.063 ng/mL for Ce(IV) and 0.182 ng/mL for Gd(III). The LOD for Ce(IV) is approximately 76 times lower than the one obtained by spectrophotometry [52]. The sensor was also tested with increasing concentrations of one ion while the concentration of the other ion was kept fixed in order to investigate the effect of one ion on the other one in terms of the redox behavior, and for both ions, linear calibration plots were obtained. This was an indication of the weak intermolecular effects between Cu(II) and Zn(II) ions.

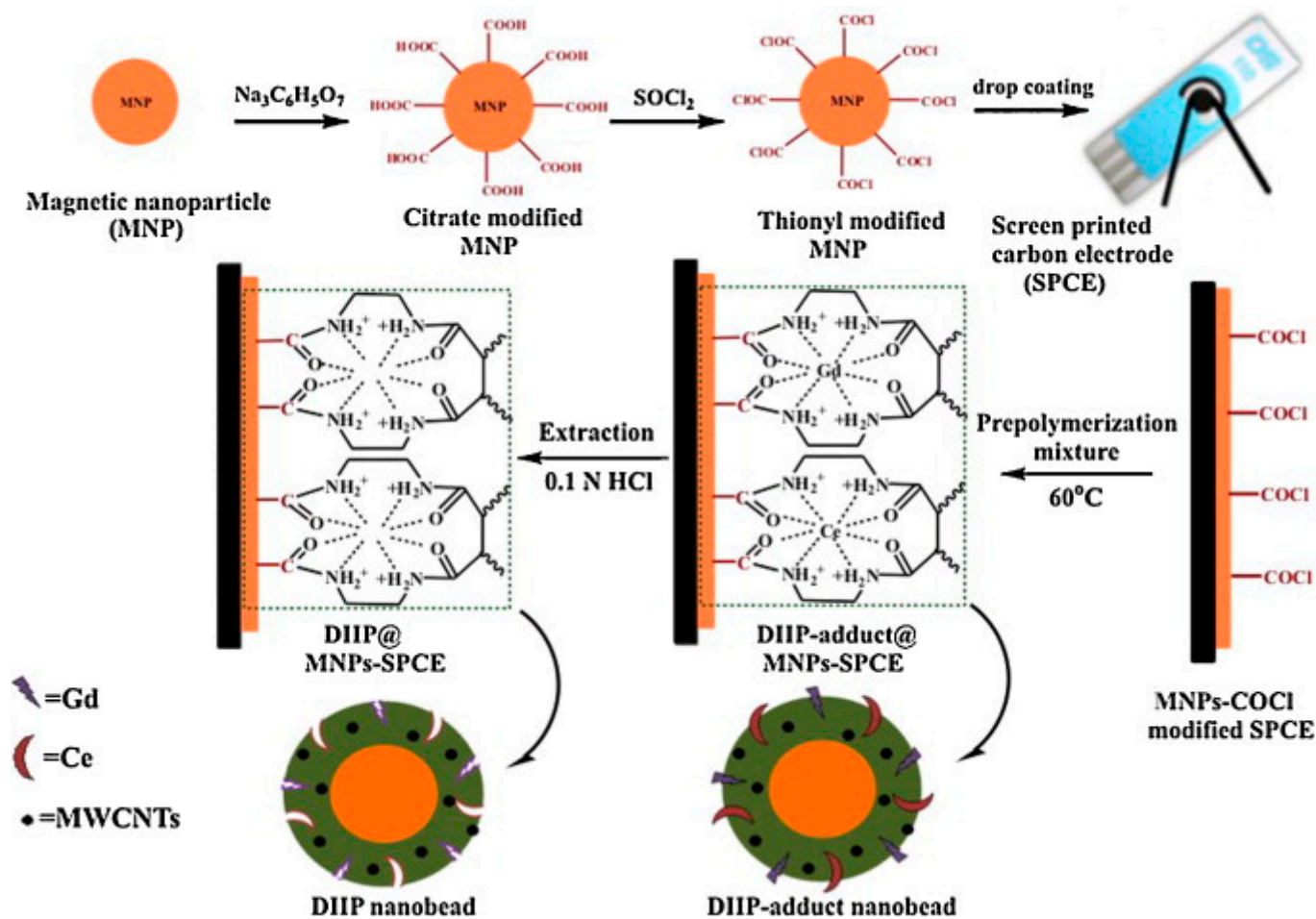


**Figure 2.** Fabrication of an ion-imprinted polymer-based screen-printed gold electrode to detect Ce(IV) and Gd(III). Reproduced with permission from [51].

Although copper and zinc are important elements for our body and immune system and have a critical effect on homeostasis and oxidative stress, they can be toxic at high concentrations [53,54]. Inductively coupled plasma mass spectrometry (ICP-MS) is considered the gold standard for trace element analysis since it has high specificity and sensitivity (ng/mL), but it has some drawbacks as it requires costly equipment and laboratory set-up, highly trained personnel and multiple high-purity gases [55]. Pencil graphite electrodes (PGEs) were used by Kumar et al. for simultaneous detection of copper and zinc [56]. In this study, important features of MWCNTs, such as high electroconductivity and good stability, were utilized and MWCNTs were mixed with bis-(2-acryloylamino-ethyl)-phosphinic acid (BAAP), Zn(II) and Cu(II), EGDMA and AIBN, which were used as the monomer, templates, cross-linker and initiator, respectively, to make the non-conducting MIP film conductive.

After thermal polymerization, the template ions were removed by an ethylenediaminetetraacetic acid (EDTA) solution. The DPASV was measured for different concentrations of both ions and 0.0159  $\mu\text{g/L}$  and 0.0275  $\mu\text{g/L}$  were obtained as the LOD in aqueous sample for Cu(II) and Zn(II), respectively. In order to evaluate the selectivity of the sensor,  $\text{Fe}^{+3}$ ,  $\text{Ca}^{2+}$ ,  $\text{Mg}^{2+}$ , nitrate, urea, ascorbic acid, and dopamine were used as interfering substances. It was observed that the produced sensor did not show any response to interfering substances. The proposed sensor for Cu(II) and Zn(II) detection may be an alternative to ICP-MS because it has an easy production process and provides as low detection limits as ICP-MS.

## 2.2. Detection of Biomarkers

The majority of biomarkers are biomacromolecules with large molecules with high molecular weights (1–100 kDa), such as proteins, enzymes, and nucleic acids. While the detection of biomacromolecules is very important in various aspects, their imprinting is difficult due to their large dimensions, complex structures, insolubility in organic solvents, slow mass transfer and structural flexibility in solution. These challenges can be overcome by using different imprinting methods, such as surface and epitope imprinting, using appropriate polymerization methods in which the MIP thickness can be controlled, such as electropolymerization, considering the large dimensions of the biomacromolecule, and using nanomaterials that reduce mass transfer resistance and have a large surface to volume ratio in MIPs [57–59].

The detection of small molecules such as hydrocortisone and testosterone is also vital in terms of early diagnosis, prognosis and treatment [60,61]. 8-hydroxy-20-deoxyguanosine (8-OHdG) and 3-nitrotyrosine (3-NT) are critical biomarkers: 8-OHdG is a biomarker of DNA damage and 3-NT is a biomarker of Alzheimer's and Parkinson's diseases. Nontawong et al. fabricated a dual-imprinted paper-based electrochemical sensor to detect 3-NT and 8-OHdG simultaneously [62]. Silica nanospheres modified with silver nanoparticles were used as the imprinting surface to improve the sensitivity and selectivity of the sensor because nanomaterials provide a larger surface/mass ratio and easily accessible recognition cavities (Figure 3a). Modified nanospheres were coated with L-cysteine via the thiol group and polymerized in the presence of 3-NT and guanosine (a dummy of 8-OHdG), *N*-isopropylacrylamide (NIPAM), *N,N*-(1,2 dihydroxyethylene) bis-acrylamide (DHEBA) and AIBN separately, followed by template removal with methanol/acetic acid solution to produce 3-NT- and 8-OHdG-based MIPs. In the paper-based sensor fabrication step, hydrophobic barrier layers were printed on filter paper to create three-dimensional circular reservoirs (Figure 3b). Four electrodes (two electrodes as working electrodes for 3-NT and 8-OHdG, reference and counter electrodes) were then fabricated and assembled on filter paper for electrochemical detection. In order to fabricate working electrodes, graphene ink was mixed with 3-NT- and 8-OHdG-based MIPs. The performance of the sensor was evaluated by square wave voltammetry (SWV). For detection, 3-NT and 8-OHdG showed well-defined oxidation peaks and the current responses increased with the increasing concentration of both templates. The LODs were determined as 2.7 nM for 3-NT and 13.8 nM for 8-OHdG—lower than in previous studies [63–65]—with wide linear dynamic ranges.

An electrochemical sensor for the simultaneous detection of carbohydrate antigen 72-4 (CA72-4) and carbohydrate antigen 19-9 (CA19-9) gastric cancer tumor markers was proposed by Luo et al. [66]. Detection of tumor markers was achieved via glycosyl imprinting and lectin-specific binding as a two-step detection. In the first step, the MIP was synthesized by electropolymerization of the characteristic glycopeptide STn and SLe<sup>a</sup> found on the surface of CA72-4 and CA19-9, respectively, 2-aminophenylboronic acid and aminophenylthiophenol-modified nanogold. After elution to create cavities and re-

adsorption for binding of CA72-4 and CA19-9, the secondary specific recognition of CA72-4 and CA19-9 was assessed. In the second step, SNA modified with cysteine (Cys) and AuNPs for CA72-4 and MAL modified with AuNPs and ferrocenecarboxylic acid (Fc) for CA19-9 were prepared and incubated to bind to the glycosyl groups of CA72-4 and CA19-9. Differential pulse voltammetry (DPV) was employed to evaluate the performance of Cys and Fc as redox probes. The MAL-Au-Fc probe showed excellent redox properties with well-defined redox peaks; on the other hand, the SNA-Au-Cys probe gave a sensitive oxidation peak but a weaker reduction peak. According to the CV and EIS results used to assess the sensor performance, the produced sensor recognized both tumor markers specifically in about 30 min, with 0.0041 U/mL and 0.0032 U/mL LODs for CA72-4 and CA19-9, respectively. These LOD values make the sensor a powerful candidate for CA72-4 and CA19-9 detection when compared to performance of other electrochemical sensors for the detection of both markers [67,68].

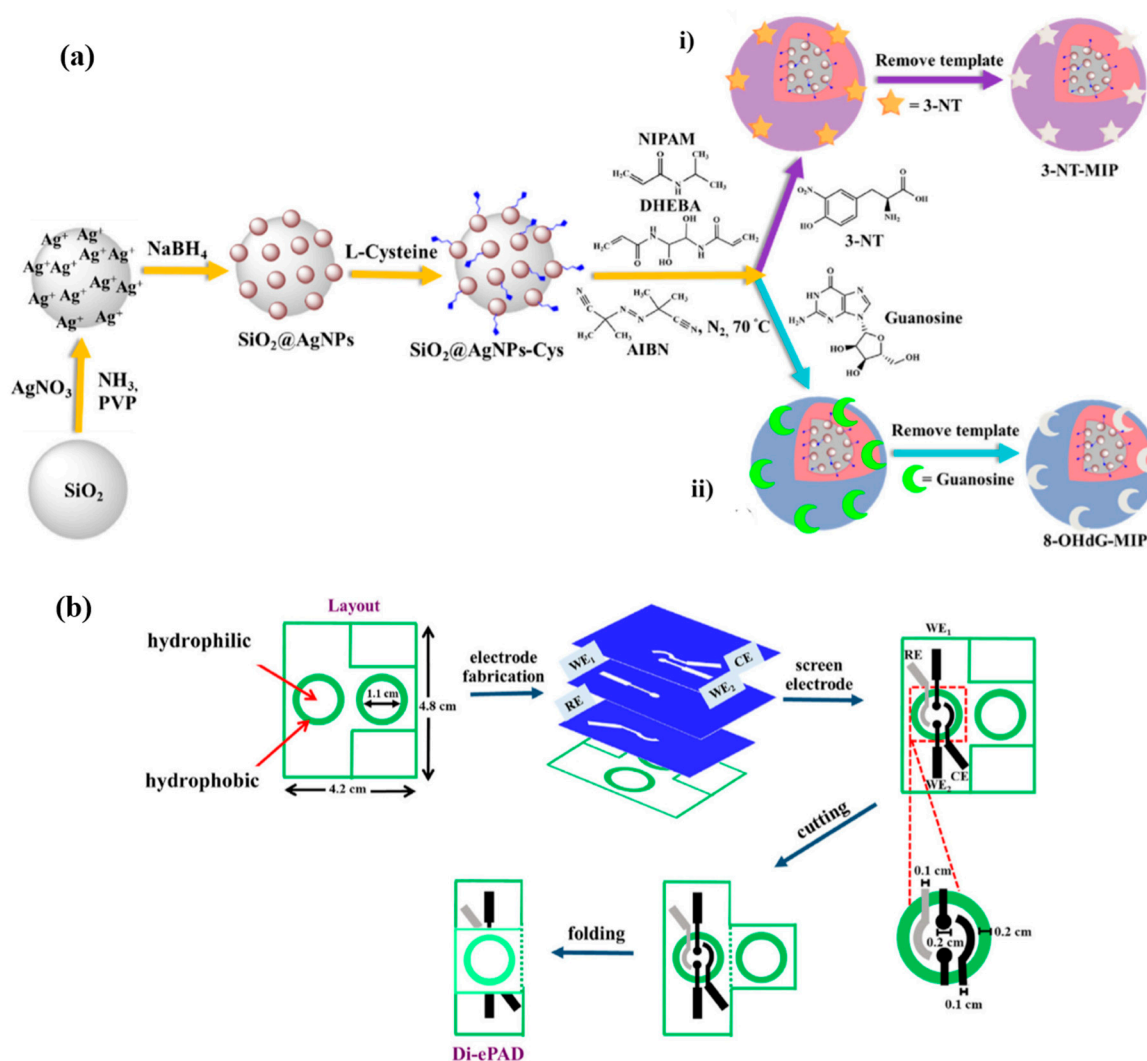


**Figure 3.** (a) Preparation of (i) 3-NT and (ii) 8-OHdG MIPs on SiO<sub>2</sub>@AgNPs-Cys obtained by the modification of SiO<sub>2</sub> with AgNO<sub>3</sub>, NaBH<sub>4</sub> and L-cysteine, respectively, before radical polymerization where 3-NT and guanosine were used as monomers. (b) Fabrication of the dual-imprinted paper-based electrochemical sensor by creating a hydrophobic reservoir on a filter paper to be used by voltametric cells by using Penguard enamel and constructing four electrodes by in-house screen printing and finally folding the spare reservoir on the electrodes to detect 3-NT and 8-OHdG. Reproduced with permission from [62].



Wang et al. produced an MIP-based electrochemical sensor to detect alpha-fetoprotein (AFP) and carcinoembryonic antigen (CEA), which are tumor markers for liver and bowel cancer in particular, respectively [69]. In this study, metallic labels were prepared by removing iron from recombinant ferritin to form apoferritin (r-Apo) and adding  $\text{Cd}^{2+}$  and  $\text{Pb}^{2+}$  and mixing with a graphene–Au composite. Finally, it was incubated with primary antibodies solution. Dual-template magnetic MIP (DT-MMIP) was prepared by polymerization of AFP and CEA and dopamine on  $\text{Fe}_3\text{O}_4$  nanoparticles and removal of AFP and CEA by SDS solution. For electrochemical detection, DT-MMIP was incubated with AFP and CEA and dispersed into metallic label solution. The SWV results showed that the anodic peak currents of  $\text{Cd}^{2+}$  and  $\text{Pb}^{2+}$  increased with increasing concentrations of tumor markers. The LOD values were 0.3 and 0.35 pg/mL for AFP and CEA, respectively, which are at least ten times lower than in the study where AFP and CEA were detected simultaneously by an electrochemical assay [70].

Another study on the detection (one-by-one) of AFP and CEA by a dual-template molecularly imprinted polymer (DT-MIP) was conducted by Taheri et al. [71]. The sensor was established on a fluorine-doped tin oxide (FTO) electrode by electropolymerizing methyl orange (MO), AFP, CEA and pyrrole (Py) and removing AFP and CEA with NaOH. In the one-by-one detection method, DT-MIP was exposed to CEA until no more  $R_{ct}$  changes observed in the EIS. Thus, all the CEA-specific cavities were occupied by CEA and afterward DT-MIP was incubated with AFP many times until it gave a linear regression after EIS measurements. For the determination of CEA, DT-MIP was washed with NaOH to remove both templates and exposed to AFP for occupation of the AFP-specific cavities. Subsequently, CEA detection was carried out. The CV and EIS results confirmed that polypyrrole (PPy) and MO increased the conductivity as after the polymerization of them, the current increased in CV and the  $R_{ct}$  decreased in EIS. After incubation with AFP and CEA since the cavities were occupied by AFP and CEA, CV showed lower current as a result of bare electron transfer and EIS displayed higher impedance as a consequence of higher resistance of the double layer. DT-MIP had the detection limits of 1.6 pg/mL for CEA and 3.3 pg/mL for AFP. These are satisfactory results in comparison to the LODs obtained by electrochemical immunosensors [69,72,73].

Prostate-specific antigen (PSA) and myoglobin (Myo) are both proteins and biomarkers of prostate cancer. It is acknowledged that their high concentration in men's blood is an indicator of prostate cancer. Their detection is very important to diagnose the cancer at early stages. In accordance with this purpose, Karami et al. constructed an antibody molecularly imprinted polymer-based immunosensor to detect prostate-specific antigen and myoglobin markers [74]. Gold screen-printed electrodes (SPE) were modified with 3,3'-dithiodipropionic acid di(N-hydroxysuccinimide ester) (DSP) and PSA and Myo were attached to the modified electrode surface via covalent bonds. Subsequently, polymerization was carried out in the presence of acrylamide (AM) as a monomer, N,N'-methylenebisacrylamide (NNMBA) as a cross-linker, and PSA and Myo as the templates. Oxalic acid (Oac) was selected as the elution solution to remove entrapped PSA and Myo from the polymeric matrix as it can break peptide bonds (Figure 4). For nanocomposite (NCP) synthesis,  $\text{Fe}_3\text{O}_4$ , MWCNTs, graphene oxide (GO) and PSA-specific antibody were used. EIS measurements were run at two different stages for detection of PSA and Myo. First, it was measured when the MIP was incubated with PSA and Myo. Second, it was measured when NCP was incubated with MIP, which was already incubated with PSA and Myo. This time, binding resulted from the interaction between PSA and the PSA-specific antibody. The  $R_{ct}$  difference between two EIS measurements was attributed to Myo binding. After the EIS results, it was confirmed that the MIP-based sensor is highly sensitive, with 5.4 pg/mL and 0.83 ng/mL LODs for PSA and Myo, respectively, well below the required

clinical range [75]. Moreover, NCP is a proper sensing interface for PSA detection with high conductivity.

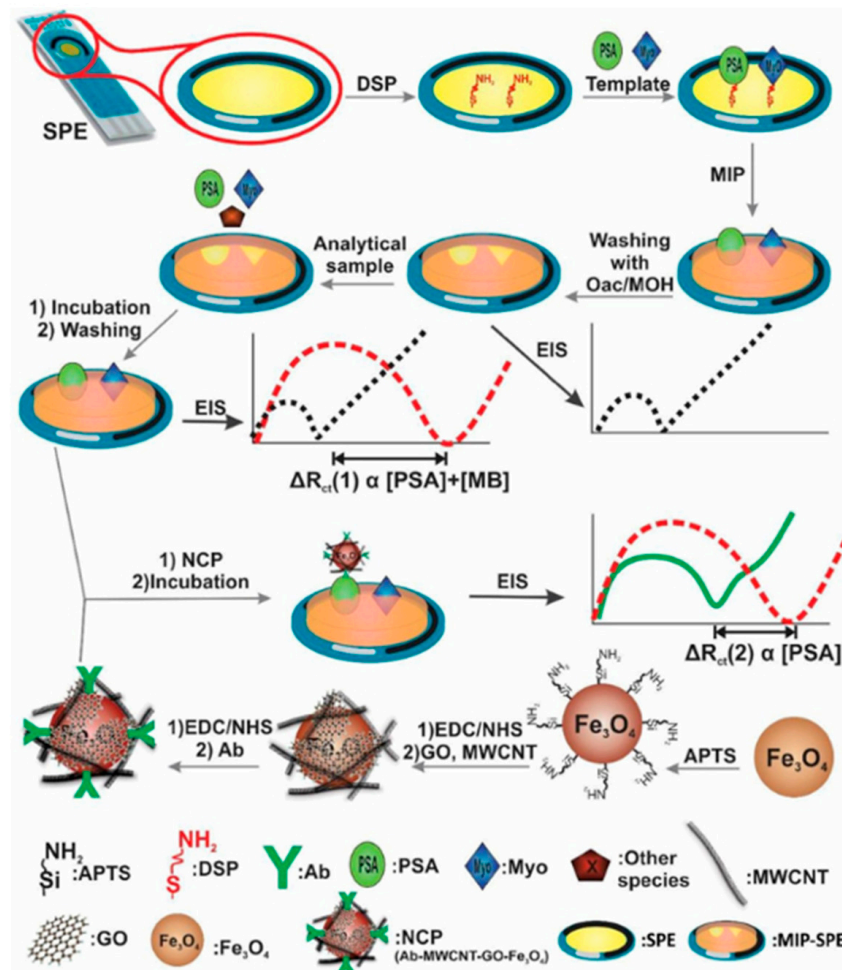


**Figure 4.** Schematic illustration of the process of MIP and NCP synthesis, along with the detection of PSA and Myo using EIS after incubating the sensor with PSA and Myo, and the NCP-PSA antibody, respectively. Reproduced with permission from [74].

Epidermal growth factor receptor (EGFR) and vascular endothelial growth factor (VEGF) are valuable cancer biomarkers that can provide important information for early cancer diagnosis. For simultaneous detection of these biomarkers, Johari-Ahar et al. developed a biosensor consisting of MIPs and antibody-conjugated nano-liposomes [76]. The MIPs were prepared in the same way and using the same chemicals as the MIP in the above article [74], except utilizing EGFR and VEGF as templates in this study. Antibody-conjugated nano-liposomes were designed by preparation of Cu(II)- and Cd(II)-loaded liposomes and conjugation of EGFR- and VEGF-specific antibodies with Cd(II)- and Cu(II)-loaded liposomes, respectively. Before evaluating the performance of the sensor, it was exposed to EGFR and VEGF and then incubated with antibody-conjugated nano-liposomes. EIS measurements showed that the created cavities were specific for EGFR and VEGF as the  $R_{ct}$  increased with the incubation of the biomarkers and the use of antibody-conjugated nano-liposomes amplified the electrochemical signal. The LODs were calculated to be 0.01 pg/mL for EGFR and 0.005 pg/mL for VEGF. The high sensitivity, selectivity and reproducibility of the proposed sensor make it a superior candidate among other electrochemical sensors produced for EGFR and VEGF detection [77–79].

Pandey et al. introduced a nanocube-shaped dual imprinted polymer-based electrochemical sensor for the detection of hemoglobin (Hb) and glycosylated hemoglobin (HbA1c), which are biomarkers of gestational diabetes mellitus [80]. In the sensor fabrication process, 3-amino-phenyl boronic acid (APBA), rhodamine b, HbA1c and Hb were electropolymerized on the carbon-paste-coated aluminum foil. During electropolymerization, APBA and rhodamine b were attached to each other via amide bonds; on the other hand, HbA1c and Hb were bound to a boronic acid moiety via a cis-diol bond of glucose and attached to a rhodamine b moiety via H-bonding with the presence of amino acid groups of Hb. HbA1c and Hb were extracted electrochemically. The sensor performance was analyzed both individually and simultaneously by DPV. In both individual measurements, the DPV responses increased linearly with an increase in the concentration of HbA1c and Hb. For simultaneous determination of HbA1c and Hb, DPV showed a regression linear curve for both biomarkers. Furthermore, well-defined separate peaks were obtained at their respective potentials, as determined during individual DPV measurements. The sensor demonstrated very low LODs (0.084 ng/mL for Hb and 0.095 ng/mL for HbA1c) as well as being very flexible, with the electrochemical response remaining unchanged despite being bent 450 times.

Immunoglobulins sometimes act as a biomarker and provide important information about health. Detection of the antibodies produced in the first and later stages of diseases is clinically important in terms of early diagnosis of the disease, determining its stage and identifying the treatments that need to be applied. Liu et al. proposed a dual molecularly imprinted polymer-based electrochemical sensor to detect IgG and IgM, where AuNPs, GO and MWCNTs were utilized to enhance the electrochemical signals and increase the stability of the signal probes [81]. Electropolymerization of Py was followed by template removal with acetic acid and SDS solution. The produced sensor had very low LODs, with 28.80 pg/mL for IgG and 0.58 pg/mL for IgM, and showed high selectivity toward a mixture of other substances, such as BSA, HGB, L-Trp and D-Tyr.

Overviews of the imprinted MT-MIP-based electrochemical sensors developed for the detection of ions and biomacromolecules are presented in Tables 1 and 2, respectively.

**Table 1.** Summary of ion-imprinted MT-MIP-based electrochemical sensors.

Template	MIP Components	Elution Solution	Electrochemical Method	Linear Range	LOD	Application	Ref.
Cd(II) Cu(II)	AEDP, L-histidine, EGDMA, AIBN	EDTA	DPASV	0.124–2.989 ng/mL 0.124–0.725 ng/mL	0.053 ng/mL 0.035 ng/mL	Human blood serum Cow's milk Lake water	[47]
Ce(IV) Gd(III)	But-2-enedioic acid bis-[(2-aminoethyl)-amide], EGDMA AIBN	HCl	DPASV	0.27–5.35 ng/mL 0.75–9.45 ng/mL	0.063 ng/mL 0.182 ng/mL	Water Human serum	[51]
Cu(II) Zn(II)	BAAP, EGDMA, AIBN	EDTA	DPASV	0.098–23.80 µg/L	0.0159 µg/L 0.0275 µg/L	-	[56]

**Table 2.** Summary of biomacromolecule-imprinted MT-MIP-based electrochemical sensors.

Template	MIP Components	Elution Solution	Electrochemical Method	Linear Range	LOD	Application	Ref.
8-OHdG 3-NT	NIPAM, DHEBA, AIBN	Methanol/ acetic acid	SWV	0.05–500 $\mu\text{M}$ 0.01–500 $\mu\text{M}$	0.0138 $\mu\text{M}$ 0.0027 $\mu\text{M}$	Urine Serum	[62]
CA72-4 CA19-9	2-aminopheny- lboronic acid	Methanol/ acetic acid	DPV	0.005–100.0 U/mL	0.0041 U/mL 0.0032 U/mL	Serum	[66]
AFP CEA	Dopamine	SDS	SWV	0.001–5 ng/mL	0.3 pg/mL 0.35 pg/mL	Human serum	[69]
AFP CEA	Pyrrole	NaOH	EIS	10–10 <sup>4</sup> pg/mL 5–10 <sup>4</sup> pg/mL	3.3 pg/mL 1.6 pg/mL	Human serum	[71]
PSA Myo	AM, NNMBBA,	Oac	EIS	0.01–100 ng/mL 1–20,000 ng/mL	5.4 pg/mL 0.83 ng/mL	Serum Urine	[74]
EGFR VEGF	AM, NNMBBA	Oac	PSA	0.05–50,000 pg/mL 0.01–7000 pg/mL	0.01 pg/mL 0.005 pg/mL	Serum	[76]
Hb HbA1c	APBA	PBS (overoxi- dation)	DPV	0.1–250 ng/mL 0.5–235 ng/mL	0.084 ng/mL 0.095 ng/mL	Blood	[80]
IgG IgM	Pyrrole	Acetic acid/SDS	DPV	0.05–500 ng/mL 0.001–100 ng/mL	0.0288 ng/mL 0.00058 ng/mL	Serum	[81]

### 2.3. Detection of Amino Acids

Amino acids are the building blocks of proteins and the most important organic molecules for organisms. They are found in two forms: levorotatory (L-) and dextrorotatory (D-) amino acids. Their detection is critical for many fields, including medicine, agriculture, and food, and also for tissue metabolism as they take part in many human body functions and sometimes act as biomarkers of different diseases.

A one-by-one detection method was adopted by Prasad et al. to detect D- and L-aspartic acid enantiomeric pairs by a dual-template molecularly imprinted polymer-based electrochemical sensor [82]. The surface “grafting from” approach was followed for sensor fabrication. After modification of a pencil graphite electrode (PGE) with AuNPs, free radical polymerization was conducted in the presence of N-acryloyl pyrrolidine-2,5-dione (NAPD, functional monomer), EGDMA (cross-linker), AIBN (initiator), D- and L-aspartic acid (templates) and MWCNTs, followed by template removal with NaOH and phosphate buffer. Although enantioselective analysis of D- and L-aspartic acid is challenging since they have same oxidation potential, the produced sensor managed to distinguish between them with 1.11 and 1.14 ng/mL LODs for D- and L-aspartic acid, respectively.

In another study to detect D-cysteine (D-Cys) and L-cysteine (L-Cys), Hou et al. used a magnetic glassy carbon electrode (MGCE), which was drop-coated with molybdenum disulfide-ionic liquid (MoS<sub>2</sub>-IL) and electrodeposited with chitosan (CS) before drop-coating with MIPs, including methacrylic acid (MAA), acrylic amide (AM), N-isopropylacrylamide (NIPAM) as monomers, N,N methylenebis(acrylamide) (MBA) as cross-linker, D- and L-cysteine as templates and Fe<sub>3</sub>O<sub>4</sub> NPs as the framework material [83] (Figure 5a). The templates were extracted with acetic acid and acetonitrile solution. Each step in the sensor fabrication was observed by CV and EIS. Electrochemical detection was carried out by DPV through a one-by-one detection method (vector method) as the oxidation potential of both templates overlaps. The DPV results revealed that the sensor was able to detect D- and L-cysteine by a one-by-one detection method, which allows the detection of one target after the sensor is saturated with the other target (Figure 5b). The LODs of

L-Cys and D-Cys were 0.7402 pg/mL and 0.6136 pg/mL, respectively. In comparison to the reported electrochemical chiral detection of L-Cys and D-Cys, the produced sensor showed higher sensitivity, which can be attributed to the outstanding electrical conductivity and large surface area of MoS<sub>2</sub>-IL [84,85].

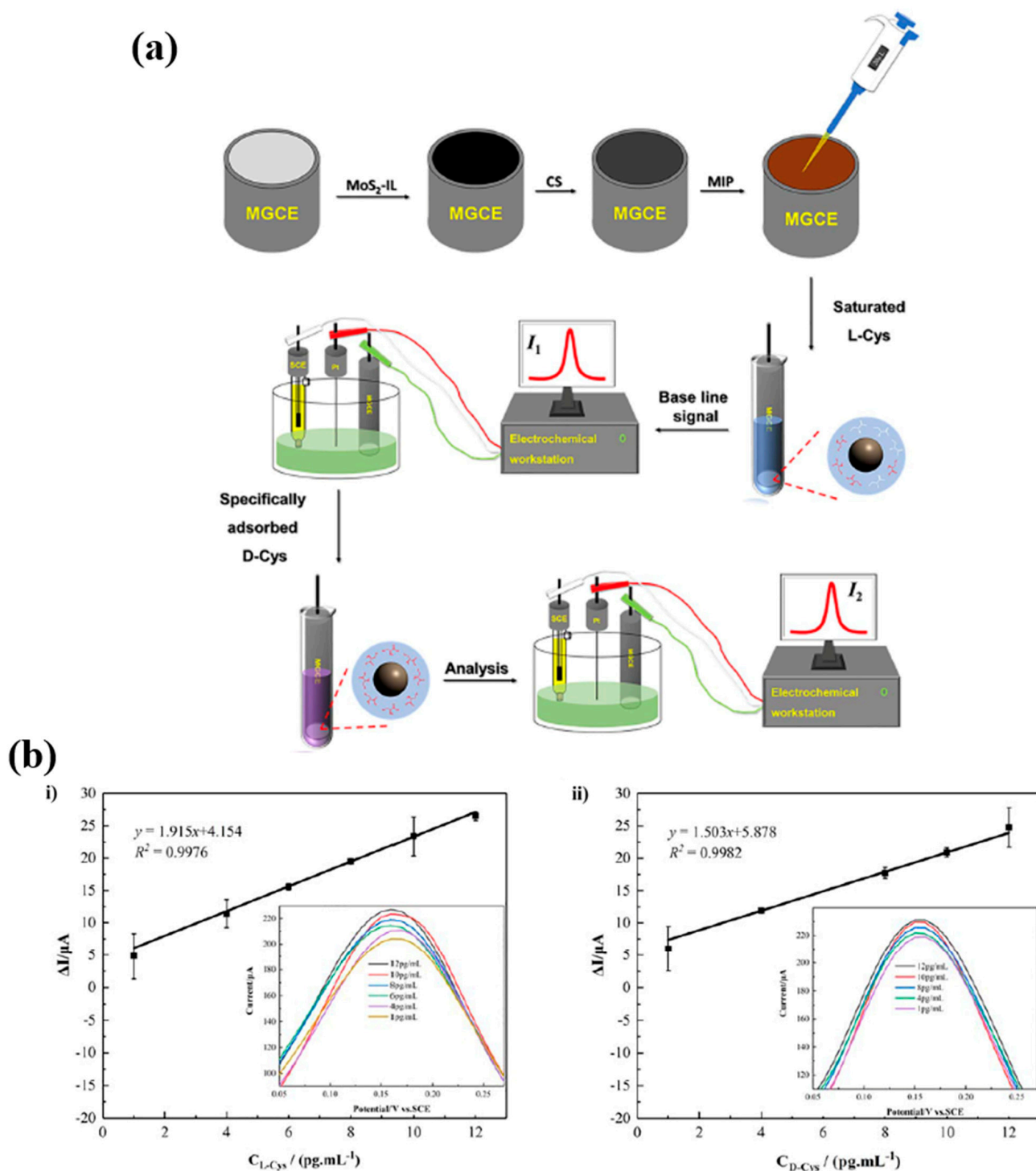


**Figure 5.** (a) Schematic illustration of the preparation of MIP/MoS<sub>2</sub>-IL/CS/MGCE and the set-up for electrochemical enantioanalysis of D-Cys and L-Cys, and (b) the linear relationship between the current response and the L-Cys concentration (i) and D-Cys concentration (ii) (insets: DPV responses for L-Cys (i) and D-Cys (ii)). Reproduced with permission from [83].



#### 2.4. Detection of Pharmaceutical Compounds

Pharmaceuticals are drugs used to treat diseases, reduce symptoms, or stop the progression of disease after its initial stages. While their use in low doses may cause the treatment to be ineffective, their use in high doses may be toxic or cause adverse side effects [86]. The effectiveness of pharmaceuticals depends on the dose used as well as the impurities of the pharmaceuticals [87]. Pharmaceuticals should be impurity-free as impurities may reduce the effectiveness of the drug. For all these reasons, the monitoring, detection and quantification of pharmaceuticals are important for patient health. Different analytical techniques, such as chromatographic, gravimetric and spectroscopic techniques, can be used for these purposes, but the advantages of MIPs over these methods make it a powerful technique and different pharmaceuticals have been detected by MIPs.

Chlorambucil (Chb) is used for cancer treatment and dacarbazine (Dac) is used for malignant melanoma, Hodgkin's lymphoma and soft tissue sarcoma. They both have similar side effects, and to avoid these, their dosage should be adjusted carefully, and this reveals the need for a sensor for their analysis and detection. By use of acryloylated tetraamine cobalt phthalocyanine (aTACoPC) as a crosslinking monomer, a dual imprinted polymer-based electrochemical sensor was fabricated on a reduced graphene oxide ceramic electrode (rGOCE) by Fatma et al. to detect Chb and Dac [28]. During the DT-MIP synthesis process, Chb, Dac, aTACoPC and AIBN were mixed to form a prepolymer mixture and spin-coated on an rGOCE, followed by free radical polymerization. Finally, the rGOCE was dipped in acetonitrile-methanol solution to retrieve Chb and Dac. The DPASV results showed that the sensor with a high imprinting factor could differentiate and detect both templates simultaneously and successively. The sensor had good stability as no deviation in current was observed over more than one month. Additionally, five electrodes produced under similar conditions gave identical responses by the DPASV measurements, indicating the reproducibility of the sensor.

Antipyrine (AnP) and ethionamide (ETH) are nonsteroidal anti-inflammatory drugs used for clinical applications to reduce pain and as an antibiotic used for tuberculosis treatment, respectively. Their overdose usage can result in multiple side effects. The sensor developed by Singh et al. detected AnP and ETH sensitively [88]. Reduced graphene oxide (RGO) was prepared and drop-coated on a glassy carbon electrode (GCE). A prepolymerization solution was prepared with 3-thiophene acetic acid (3-TAA), AnP and ETH in phosphate-buffered saline (PBS) and electropolymerization was performed by CV. Afterwards, the MIP-modified GCE was eluted with methanol-acetic acid solution to remove AnP and ETH and create cavities complementary in size and shape to AnP and ETH. The MIP-based GCE sensor was evaluated using  $K_3[Fe(CN)_6]$  as a redox probe by CV. Because 3-TAA has insulating properties, the current response decreased after electropolymerization, but with the removal of AnP and ETH, the current increased as cavities were created. The performance of the sensor in terms of the detection of AnP and ETH individually was assessed by DPV. The LODs were found to be 0.117  $\mu$ M for AnP and 0.15  $\mu$ M for ETH. When compared to other sensors produced for AnP and ETH detection, these low LODs can be attributed to the higher conductivity of RGO, which is used in electrochemical sensors to increase the sensitivity of target detection [89,90].

Sulfadiazine (SDZ) and acetaminophen (AP) were detected simultaneously by an electrochemical sensor as their excessive consumption is harmful. Sun et al. firstly modified GCE with a highly conductive graphene oxide@covalent organic framework composite (GO@COF) [91]. SDZ, AP, pyrrole and tetrabutyl ammonium perchlorate (TBAP) were electropolymerized in acetonitrile. Subsequently, polypyrrole was overoxidized in NaOH solution for template extraction. First, all the SDZ and AP were detected individually, with oxidation peaks at 0.36 V and 0.86 V for AP and SDZ, respectively. Following this, the

sensor was incubated with AP and SDZ at the same time for simultaneous detection and two distinct oxidation peaks were observed at 0.36 V and 0.86 V. It was determined that the current response increased with increasing AP and SDZ concentrations and this revealed a strong linear relationship between the current and the analyte concentration. The sensor also demonstrated good selectivity, accuracy, and stability for AP and SDZ detection with a wide range of concentrations and low LODs.

### 2.5. Detection of Neurotransmitters

Neurotransmitters are endogenous chemicals called messengers of the body that amplify, transmit and convert signals in cells [92]. Neurotransmitters are of great importance for human health and any imbalance in the level of neurotransmitters or the absence of neurotransmitters leads to various neurological and mental diseases, such as Alzheimer's and Parkinson's diseases [93]. Therefore, their detection and concentration determination are very important for the treatment of diseases. Since different neurotransmitters have very similar redox potentials for *in vivo* detection, it is difficult to detect them simultaneously by electrochemical methods [94]. Despite having similar redox potentials, this issue can be tackled by using MIPs due to their target-specific cavities.

Dopamine (DA) and epinephrine (EP) were detected by a three-dimensional hybrid network consisting of a molecularly imprinted polymer and MWCNTs [95]. In this study, where poly(9-carbazoleacetic acid) was synthesized and used as a functional monomer for the first time, for the simultaneous detection of DA and EP, although DA and EP have the same molecular structure, EP was used as a pseudo-template for MIP preparation since DA is a little smaller than EP and DA-imprinted MIP cavities do not let EP enter the cavities, leading to low sensitivity. After modification of GCE with MWCNT 9-carbazoleacetic acid, EP was electropolymerized on the electrode, followed by NaOH washing and ethanol for EP extraction. The advantage of using 9-carbazoleacetic acid provided enough covalent interactions with both templates and MWCNTs, which created a high specific surface area and a high conductivity sensor, resulting in low LODs of 0.015  $\mu\text{M}$  for DA and 0.023  $\mu\text{M}$  for EP, with high selectivity and sensitivity.

Another study on the detection of DA and EP was conducted by Fatma et al. [96]. Firstly, graphene oxide/carbon black composite (GO/CB) was prepared. Acryloylated-GO/CB (aGO/CB) was then synthesized and used as a crosslinking monomer. After free radical polymerization of the crosslinking monomer, DA, EP and AIBN (initiator) on SPCE, triethylamine (TEA)-methanol solution removed DA and EP from the polymer matrix and a one monomer dual imprinted polymer (OMNiDIP) was created (Figure 6a). The effect of each modification on the detection of DA and EP was assessed by DPASV. According to the results, the GO/CB composite significantly improved the response of the sensor when compared to CB and GO separately, but it was not enough to differentiate both templates (Figure 6b). After employing the MIP, the GO/CB composite sensor managed to differentiate DA and EP and detect them with LODs of 0.028 ng/mL for DA and 0.017 ng/mL for EP.

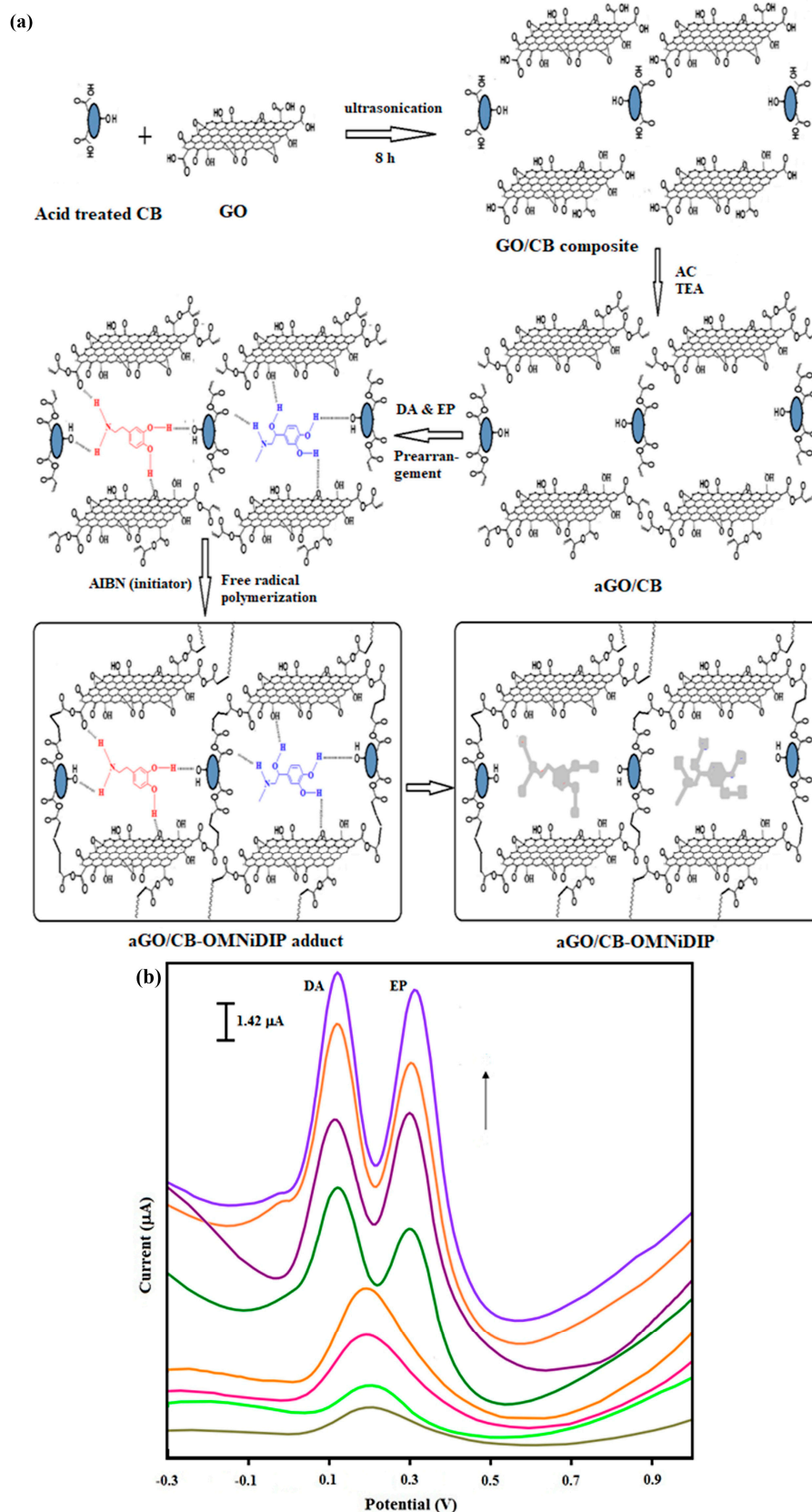


**Figure 6.** (a) Schematic protocol for the synthesis of aGO/CB-OMNiDIP, and (b) DPASV responses for DA and EP on different electrodes; from bottom to top: bare SPCE, CB/SPCE, GO/SPCE, GO/CB composite/SPCE, aCB-DIP/SPCE, aGO-DIP/SPCE, aGO/CB-DIP/SPCE and aGO/CB-OMNiDIP/SPCE. Reproduced with permission from [96].

## 2.6. Detection of Environmental Pollutants

Environmental pollutants, including chemicals, heavy metals, pesticides, herbicides, and plastics, are a threat to human health as they cause different pollutions and have adverse effects on the climate. This reveals the importance of their detection and analysis, both for global health and for the protection of the environment.

4-nitrophenol (4-NP) and hydroquinone (HQ) are both phenolic compounds that are dangerous environmental contaminants and pose a significant health threat due to their long-term aqueous stability. Thus, early detection prior to water contamination is crucial. A surface-imprinted polymeric film was fabricated on GCE for the detection of 4-NP and HQ by Singh et al. [97]. 4-amino thiophenol (4-ATP) and p-phenylenediamine (p-PD) with aromatic rings were selected as functional monomers because of their interaction with the template molecules via hydrophobic and  $\pi$ - $\pi$  interactions. The functional monomers and templates were electropolymerized in an HCl-supporting electrolyte. The templates were extracted by immersing the electrodes in methanol/water solution. After individual detection of 4-NP and p-PD, the LODs were determined as 0.14  $\mu$ M and 0.37  $\mu$ M for HQ and 4-NP, respectively. For simultaneous detection, the DPV responses were recorded for different 4-NP and HQ concentrations, and this showed two oxidation peaks at around 0.1 V (HQ) and 0.9 V (4-NP) as they were obtained at individual detection measurements. This showed that there was no interference with the templates. Additionally, lower LODs were obtained for simultaneous detection, showing that the imprinted film managed to distinguish both templates well.

In another study, platinum nanoparticle (PtNP)-decorated amino-mesoporous silica nanoparticles (MSN-PtNPs) were used as supporting material for a dual-template molecularly imprinted polymer coating for the detection of paraquat (PQ) and glyphosate (GLY), both representatives of broad-spectrum herbicides that can damage aquatic organisms if released into water systems and can cause serious health issues for humans if allowed to accumulate *in vivo*. After polymerization of PQ and GLY with acrylic acid (AA) and N-vinyl-2-pyrrolidone (VP) as monomers, DHEBA as a cross-linker, potassium peroxydisulfate ( $K_2S_2O_8$ ) as the initiator and removing the template by sonicating in water, the sensor was fabricated on a graphite electrode by manual screen-printing and modified with MIP-coated MSN-PtNPs, as shown in Figure 7. The simultaneous determination results showed that the sensor gave a linear response toward increasing concentrations of PQ and GLY; 3.1 nM and 4.0 nM were obtained as the LODs of PQ and GLY, respectively, with linear calibration curves in the range of 0.025–500  $\mu$ M for both analytes by DPV [98]. These results meet the maximum contaminant levels of PQ (0.012  $\mu$ M) and GLY (4.140  $\mu$ M) in drinking water [99,100].

Rao et al. utilized nitrogen-doped carbon nanosheet frameworks (Fe-NCNFs) decorated with Fe to be coated with MIP for simultaneous detection of mebendazole (Meb) and catechol (CC), which are environmental pollutants [101]. As Fe nanoparticles increase electrocatalytic activity and carbon nanomaterials help nanoparticles to boost their electroactivity, by taking advantage of these features, the Fe-NCNFs had larger specific surface area and fast electron transport [102,103]. Fe-NCNFs were prepared via a chemical blowing process and GCE was modified with Fe-NCNF. Meb was imprinted on the modified GCE by electropolymerization in the presence of MAA and  $LiClO_4$ , followed by the removal of Meb with acetic acid/methanol solution. The sensor detected Meb and CC, with Meb recognized through the high binding affinity of the MIP and specific cavities, and CC detected through its adsorption and electrochemical oxidation by Fe-NCNFs. The sensor has a low limit of detection of 0.06  $\mu$ M for Meb and 0.004  $\mu$ M for CC.

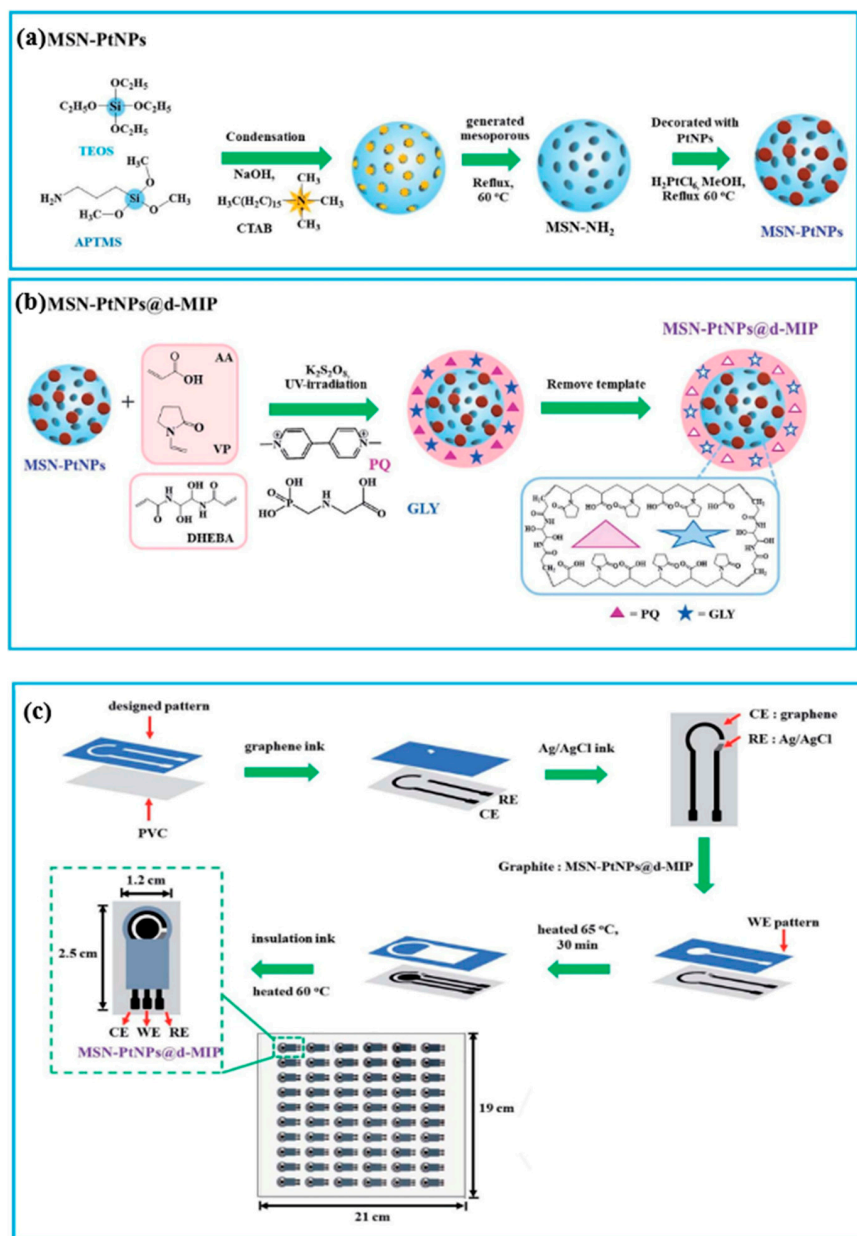


**Figure 7.** Schematic representation of synthesis of the (a) MSN-PtNPs and (b) dual imprinted MSN-PtNPs and (c) fabrication of the PQ and GLY dual-MIP sensor. Reproduced with permission from [98].

### 2.7. Detection of Cells and Viruses

Outbreaks and infections caused by bacteria and viruses have been a major concern for public health. Despite significant advancements in medical technology and treatments, as well as important developments in the field, the COVID-19 pandemic has starkly highlighted the devastating consequences of diseases caused by pathogens, which can lead to alarmingly high mortality rates. In terms of preventing diseases that bacteria and viruses cause, their early detection is of critical importance. Although many single-template MIP-based electrochemical sensors were fabricated for bacteria and virus detection [104–107], only a couple of multi-template MIP-based electrochemical sensors have been produced so far. Moakhar et al. developed a novel electrochemical sensor to detect two types of biomarkers: viral proteins from influenza A H1N1 and SARS-CoV-2, as well as specific antibodies (IgM and IgG) against SARS-CoV-2 [42]. This sensor was designed to analyze saliva samples for viral proteins and blood samples for antibodies, with the goal



of facilitating the early detection and prevention of viral respiratory infections. In this study, three 1  $\mu\text{m}$  sized gold nano/micro-sized island (NMI) electrodes, which comprise fluidic assays were electropolymerized with o-PD separately and built-in recognition sites, were created after removal with NaOH for the detection of viral particles in saliva and antibodies in blood (Figure 8c). The fluidic assay was used in an NfluidEX device, which has a multiplexed microfluidic delivery system, automated custom-made potentiostat and cartridge for sample collection (Figure 8d). NfluidEX was integrated with a smart phone via Wi-Fi and Bluetooth controllers for signal analyses and display of the results. NfluidEX showed a low limit of detection with high sensitivity and specificity and low cross-reactivity with the help of employing an NMI/MIP assay and using a proper monomer and finding high binding affinity regions between the monomer and the target proteins as a result of molecular-docking studies. The quantitative feature of the NfluidEX was evaluated by comparing it with real-time quantitative polymerase chain reaction (RT-qPCR), which is the gold standard for viruses. Patients clinically diagnosed with SARS-CoV-2 were found to be positive in both the saliva and blood tests using NfluidEX, and these results were consistent with those obtained through PCR and ELISA tests. This developed device can be used as a point-of-care device for early diagnosis to monitor and prevent the spread of viral infections due to its excellent features as it has multi-MIP detection system, allowing simultaneous detection of virus and antibodies within 11 min.

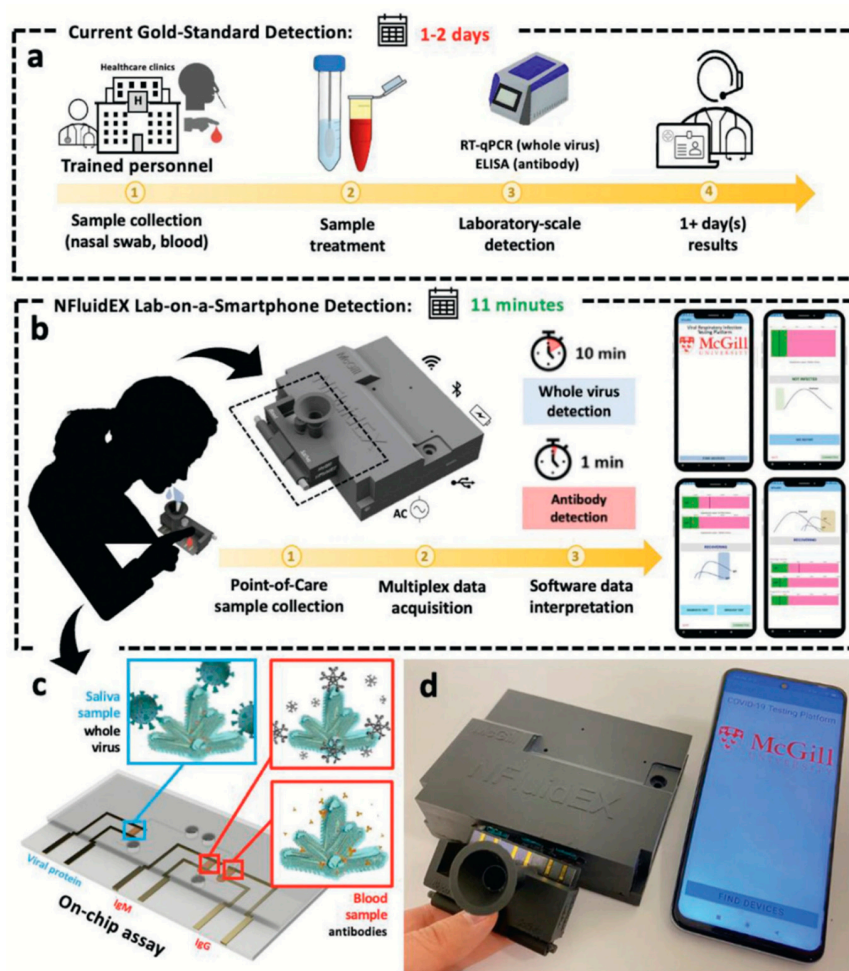


**Figure 8.** Schematic representation of the NfluidEX. (a) Current gold standard detection methods for diagnosis. (b) Steps of detection by NfluidEX. (c) On-chip assay for whole-virus detection in saliva samples and antibody detection in blood samples. (d) Real image of the NfluidEX device. Reproduced with permission from [42].

There are some challenges when imprinting whole bacteria and viruses because of their large dimensions when compared to small molecules such as nucleic acids, amino acids and proteins. For example, (i) a bulky, highly cross-linked polymer matrix may slow down the diffusion of microorganisms to the cavities as microorganisms have large dimensions; (ii) bacteria have many functional groups on their cell wall and this can make cavities hard to create and cause the heterogeneity of the binding affinity; (iii) by their nature, microorganisms can secrete various chemicals to adapt to the environment, which may cause the selectivity of the sensor to decrease; and (iv) template removal can be challenging [108,109]. These challenges can be overcome by employing different techniques and methods. For example, instead of using whole-cell imprinting, the surface components of microorganisms such as epitope and lipopolysaccharide can be imprinted, or in case of whole-cell imprinting, suitable and facile methods should be chosen [109].

When developing an MIP-based sensor for microorganism detection, due to the complex dimensions and size, the thickness of the polymer film is important and therefore the electropolymerization method, where the thickness of the MIP film can be easily controlled, is generally preferred. Moreover, electropolymerization is also advantageous as microorganisms are doped directly into the polymer matrix, which creates cavities with high affinity [110].

Since bacteria have many functional groups exposed on their surface, monomer selection is crucial for both the imprinting and the template removal processes. Dopamine [111], APBA [112] and pyrrole [113,114] are commonly used monomers. Dopamine has many functional groups, such as phenyl, amino, and hydroxyl groups, that can react with bacteria [115]. 3-aminophenylboronic acid (3-APBA) has a boronic acid group and it can specifically interact with cis-diol, which presents on the bacterial surface [104]. Pyrrole has excellent properties, including low nonspecific adsorption, good conductivity, superior stability, efficient polymerization at mild conditions and an N–H interaction that ensures high selectivity [116].

Although it is difficult to remove microorganisms from polymeric films, a variety of different useful methods are available. Acidic solutions and surfactants [117], enzyme treatment, overoxidation [118], multistep extraction procedures, including enzyme treatment, the use of surfactant and overoxidation [105,112] have been used for the removal of microorganisms.

Although the detection of microorganisms is more difficult than the detection of small molecules due to the reasons mentioned above, multiplexed detection can be achieved by using an appropriate monomer, eluent solution and imprinting method [109,119].

*Escherichia coli* (*E. coli*) O157:H7 and *Staphylococcus aureus* (*S. aureus*) are pathogenic bacteria, and they have caused many outbreaks that caused several illnesses [120–122]. Their detection is of great importance to prevent outbreaks and protect public health. A dual-bacteria-imprinted polymer (DBIP) sensor was reported by Xu et al. for *E. coli* O157:H7 and *S. aureus* detection [123]. In the DBIP preparation process, o-PD was electropolymerized on the GCE by CV in the presence of *E. coli* O157:H7 and *S. aureus*; subsequently, both bacteria were eluted by soaking the modified GCE in cetyltrimethylammonium bromide/acetic acid (CTAB/Hac) solution for 10 min. Quantitative detection of *E. coli* O157:H7 and *S. aureus* was performed separately by incubating modified GCE with both bacteria individually and measured using EIS. The LODs of the sensor were obtained as 9.4 CFU/mL for *E. coli* O157:H7 and 9.5 CFU/mL for *S. aureus*. *E. coli* O6 and *S. hemolyticus* were used as interference bacteria to test the selectivity of the sensor and the highest EIS responses were observed for *E. coli* O157:H7 + *S. aureus* and a mixture of interference bacteria + *E. coli* O157:H7 + *S. aureus*, indicating that the sensor was not affected by closely related strains (interference bacteria). As the sensor has a short fabrication time (20 min), high selectiv-

ity and sensitivity, it can be a promising tool to monitor and detect multiple pathogenic bacteria simultaneously.

An overview of the imprinted MT-MIP-based electrochemical sensors developed for the detection of organic molecules and pathogens are presented in Tables 3 and 4, respectively. Other MT-MIP-based sensors for a range of analytes, not discussed in this review, are presented in Table 5.

**Table 3.** Summary of organic-molecule-imprinted MT-MIP-based electrochemical sensors.

Template	MIP Components	Elution Solution	Electrochemical Method	Linear Range	LOD	Application	Ref.
D-aspartic acid L-aspartic acid	NAPD, EGDMA, AIBN	NaOH/ Phosphate buffer	DPASV	3.89–66.23 ng/mL 3.99–66.12 ng/mL	1.11 ng/mL 1.14 ng/mL	CSF Blood serum Pharmaceutical samples	[82]
D-Cys L-Cys	MAA, AM, NIPAM, MBA	Acetic acid/ Acetonitrile	DPV	1–12 pg/mL	0.6136 pg/mL 0.7402 pg/mL	Fetal bovine serum	[83]
Chb Dac	aTACoPC, AIBN	Acetonitrile/ Methanol	DPASV	0.159–28.524 ng/mL 0.069–35.278 ng/mL	0.037 ng/mL 0.016 ng/mL	Blood serum Urine Pharmaceutical samples	[28]
AnP ETH	3-TAA	Methanol/ Acetic acid	DPV	0.05–0.6 $\mu$ M 0.03–1.2 $\mu$ M	0.117 $\mu$ M 0.15 $\mu$ M	Human blood serum	[88]
SDZ AP	Pyrrrole, TBAP	NaOH (Overoxidation)	DPV	0.5–200 $\mu$ M 0.05–20 $\mu$ M	0.16 $\mu$ M 0.032 $\mu$ M	Pork Chicken	[91]
DA EP	9-carbazol- eacetic acid	NaOH/ Ethanol	DPSV	0.04–70 $\mu$ M	0.015 $\mu$ M 0.023 $\mu$ M	Rat plasma	[95]
DA EP	aGO/CB, AIBN	TEA/ Methanol	DPASV	0.12–4.578 ng/mL 0.075–1.188 ng/mL	0.028 ng/mL 0.017 ng/mL	Blood serum Urine Pharmaceutical samples	[96]
4-NP HQ	4-ATP, p-PD	Methanol/ Water	DPV	0.8–200 $\mu$ M	0.37 $\mu$ M 0.14 $\mu$ M	Water (distilled, packaged, tap, river)	[97]
PQ GLY	AA, VP, DHEBA, K <sub>2</sub> S <sub>2</sub> O <sub>8</sub>	Sonication in water	DPV	0.025–500 $\mu$ M	0.0031 $\mu$ M 0.004 $\mu$ M	Water (reservoir, pond, wastewater)	[98]
Meb CC	MAA, LiClO <sub>4</sub>	Methanol/ Acetic acid	DPV	0.01–1.5 $\mu$ M 0.5–25 $\mu$ M	0.004 $\mu$ M 0.06 $\mu$ M	Water (tap, river)	[101]

CSF: Cerebrospinal fluid.

**Table 4.** Summary of cell- and microorganism-imprinted MT-MIP-based electrochemical sensors.

Template	MIP Components	Elution Solution	Electrochemical Method	Linear Range	LOD	Application	Ref.
Viral particles IgG IgM	o-PD	NaOH	EIS	$9.60 \times 10^3$ – $3.84 \times 10^8$ particles/mL $10^1$ – $10^4$ pg/ $\mu$ L $10^1$ – $10^4$ pg/ $\mu$ L	2091.6 particles/mL 3.63 pg/ $\mu$ L 2.79 pg/ $\mu$ L	Saliva Plasma Blood	[42]
<i>E. coli</i> O157:H7 <i>S. aureus</i>	o-PD	CTAB/HAc	EIS	-	9.4 CFU/mL 9.5 CFU/mL	Apple juice	[123]

**Table 5.** Additional MT-MIP-based sensors for the detection of different targets.

Template	MIP Components	Elution Solution	Electrochemical Method	Linear Range	LOD	Application	Ref.
NE UA	TAT, AIBN	TEA/ Methanol	DPASV	2.98–40.69 ng/mL 1.94–43.59 ng/mL	0.66 ng/mL 0.44 ng/mL	Blood serum Urine Pharmaceutical samples	[124]
HQ CC	Melamine	Ethanol/ Water	DPV	10–100 $\mu$ M (for both)	3.1 $\mu$ M 3.5 $\mu$ M	River water	[125]
AA DA	TAT, EGDMA	ACN/ TEA	DPASV	8.28–77.92 ng/mL 0.10–5.24 ng/mL	2.21 ng/mL 0.22 ng/mL	CSF Blood serum Pharmaceutical samples	[29]
CA TPH	L-arginine	NaOH	DPV	0.01–1.0 $\mu$ M 0.1–100.0 $\mu$ M	1.3 nM 20.0 nM	Green tea Urine	[126]
UA Tyr	AMT	Ethanol	DPV	0.01 $\mu$ M–100 $\mu$ M 0.1 $\mu$ M–400 $\mu$ M	0.0032 $\mu$ M 0.046 $\mu$ M	Serum Urine	[127]
AA Tyr	m-DB, o-AP	Nitric acid	DPV	0.1–300 $\mu$ M 0.01–180 $\mu$ M	0.03 $\mu$ M 0.003 $\mu$ M	Human serum	[128]
CLB RAC	o-PD	NaOH (overoxidation)	CV	1 pM–8 nM (for both)	0.303 pM (for both)	Urine Raw pork CLB tablets	[129]
OX DZ	MAA, EGDMA, AIBN	Methanol/ Acetic acid	DPV	0.01–200 $\mu$ M 0.05–150 $\mu$ M	59 nM 21 nM	Urine Tablet	[130]
GLY GLU	EGDMA, TEA	Acetonitrile/ TEA	DPASV	3.98–176.23 ng/mL 0.54–3.96 ng/mL	0.35 ng/mL 0.19 ng/mL	Soil Human serum	[30]
Adrenaline UA	Dopamine, PBS	Methanol/ Acetic acid	OECS	0.5 pM–10 $\mu$ M 1 pM–1 mM	1 pM (for both)	Urine	[131]
CFZ AVI	o-PD, PBS	NaOH (overoxidation)	SWV	50–1000 $\mu$ M 1–1000 $\mu$ M	35 $\mu$ M 0.5 $\mu$ M	Human serum Rabbit	[132]
RIF INZ	Pyrrole	Methanol/ Water	AdSDPV	0.08–85 $\mu$ M (for both)	0.287 nM 0.371 nM	Pharmaceutical samples Blood serum Urine	[133]

Table 5. Cont.

Template	MIP Components	Elution Solution	Electrochemical Method	Linear Range	LOD	Application	Ref.
DA Chlorpromazine	Nicotinamide	Methanol/ Acetic acid	DPV	0.05–8 $\mu\text{M}$ / 8–40 $\mu\text{M}$ 0.005–2 $\mu\text{M}$	2.8 nM 0.25 nM	Human serum Urine Pharmaceutical sample	[41]
DA UA	o-PD, PBS	H <sub>2</sub> SO <sub>4</sub> (overoxidation)	DPV	2.0–180 $\mu\text{M}$ 5.0–160 $\mu\text{M}$	0.3 $\mu\text{M}$ 0.4 $\mu\text{M}$	Bovine serum	[134]
DA Ade	AM	PBS (overoxidation)	DPV	0.6–200 $\mu\text{M}$ 0.4–300 $\mu\text{M}$	0.12–0.37 $\mu\text{M}$ 0.15–0.36 $\mu\text{M}$	Human serum	[135]
NPX MTH OMZ	MAA, EGDMA, AIBN	Acetic acid/ Ethanol	DPV	5.0 nM–100 $\mu\text{M}$ 1.0 nM–130 $\mu\text{M}$ 5.0 nM–100 $\mu\text{M}$	1.0 nM 0.7 nM 1.5 nM	Human plasma Urine Tap water Tablet	[136]

NE: Norepinephrine, UA: Uric acid, TAT: 2,4,6-trisacrylamido-1,3,5-triazine, Ery: Erythromycin, Cla: Clarithromycin, Azi: Azithromycin, mPD: m-phenylenediamine, AA: Ascorbic acid, CA: Catechin, TPH: Theophylline, G: Guanine, X: Xanthine, Tyr: Tyrosine, AMT: 2-amino-5-mercapto-1, 3, 4-thiadiazole, m-DB: m-dihydroxy benzene, o-AP: o-aminophenol, CLB: Clenbuterol hydrochloride, RAC: Ractopamine, OX: Oxazepam, DZ: Diazepam, GLU: Glufosinate, OECT: Organic electrochemical transistor, CFZ: Cefazidime, AVI: Avibactam, RIF: Rifampicin, INZ: Isoniazid, CPZ: Chlorpromazine, Ade: Adenine, NPX: Naproxen, MTH: Methocarbamol, OMZ: Omeprazole.

### 3. Integration of Microfluidics and Commercialization

The detection of biomarkers, substances and pathogens that can affect public health and cause diseases is vital for early-stage detection and to make accurate diagnoses in a short time, which facilitates the initiation of an effective treatment regime. Current diagnostic tools have disadvantages, including the costs, requiring trained personnel, and the slow time to diagnosis, and are generally devices that are difficult to transport, preventing use in remote environments. Therefore, the need for effective point-of-care (POC) diagnostic tools is greatly increasing. POC diagnostics is a new strategy for real-time, rapid, accurate, and on-site detection at the patient's point of need, as depicted in Figure 9.

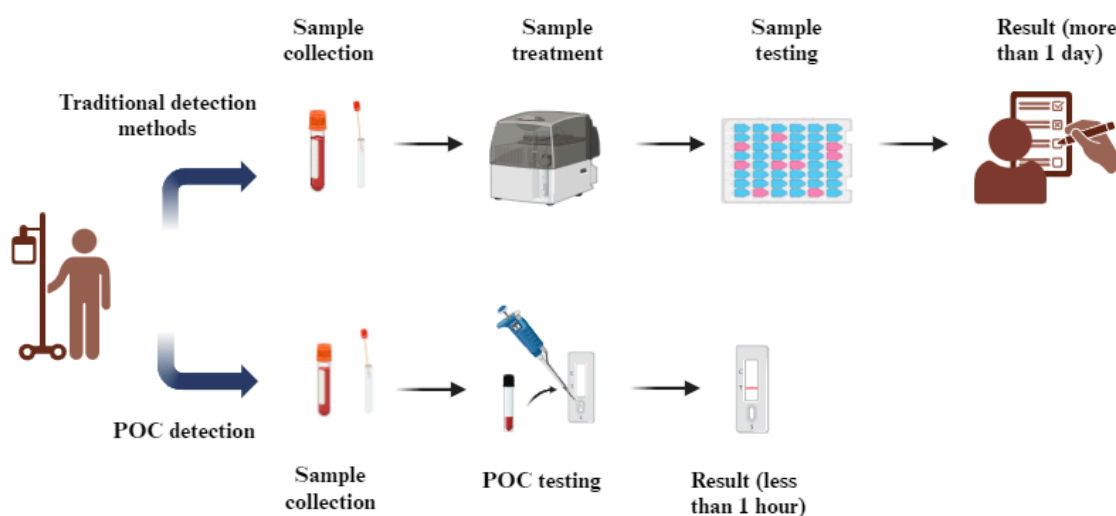


Figure 9. Schematic illustration of disease detection using traditional methods relying on centralized laboratories and POC testing approaches.



Microfluidic systems control and manipulate small amounts of liquids (typically  $\mu\text{L}$  to nL or lower) using microscale-level channels [137]. They enable smaller samples and reagents volumes, portability, precise reaction control, parallelization, high surface to volume ratio and spatio-temporal resolution [138]. MIPs with many advantages can be employed in the design of microfluidic systems for POC applications. Integration of MIPs with microfluidic devices allows an increase in sensitivity and selectivity. MIP-based microfluidic devices have been used for electrochemical detection of biomarkers [139,140], amino acids [141,142], hormones [143] and drugs [144,145].

Multiplexed detection is performed by three approaches: spatial separation of detection sites, regional separation or the use of different labels and biorecognition elements [146]. Microfluidic devices are suitable platforms for multiplexed detection because of the characteristic properties and design [147–149]. Microfluidics can have separate individual chambers for each analyte; thus, each analyte can only interact with its biorecognition element, reducing the possible cross-reactivity [150]. While complex and long processes are required for the detection of a single component and are more complicated for multiplexed detection, with microfluidic devices, the sample preparation, incubation and detection can be automated, significantly reducing complications and requiring less time [137].

Considering the benefits of microfluidics in terms of multiplexed detection, the integration of MIPs with microfluidics can lead to significant developments in the field of multiplexed detection by MIPs. Integrating MT-MIPs with microfluidic systems offers great potential for real-time analysis of target molecules in complex samples. To achieve this integration, the microfluidic device must be designed to accommodate MT-MIPs, often incorporating channels that allow for the continuous flow of sample solutions through a series of reaction zones. The MT-MIPs are typically loaded into the microfluidic channels by adsorbing them onto microbeads or directly onto the surfaces of the channels. Magnetic nanoparticles are often integrated for easy manipulation and to help remove excess template or interfere with non-specific binding [151,152]. Potential challenges for the integration of MT-MIPs within the microfluidic system are linked to the matrix interference, integration complexity and clogging of channels. To minimize the matrix effects, sample pre-treatments such as filtration and dilution can help remove large substances. Utilizing advances in droplet-based microfluidics can make it easier to control the particle size and distribution to control the integration complexity. Using hydrophilic materials can reduce the particle adhesion and optimizing the flow rate can prevent particle accumulation [152]; both methods can reduce the possibility of clogging.

The integration of MT-MIPs with microfluidic systems is also of great importance for the commercialization of MIPs. Several commercial MIP products are produced by companies such as MIP diagnostics (NanoMIPs), Sigma Aldrich (SupelMIP), Aspira Biosystems, Semorex, Affinisep and Biotage. Early commercialization of MIP products started for purification and separation applications. Biotage, Sigma Aldrich and Affinisep offer solid-phase extraction (SPE) cartridges for a broad range of applications, including healthcare, food safety and environmental analysis. Semorex and Aspira Biosystems synthesize MIPs on a large scale for detection purposes. Semorex produces MIPs for protein detection that can be further used for therapeutics for cancer [153]. MIPs synthesized by epitope imprinting are sold by Aspira Biosystems for microorganisms' detection [154]. Sixth Wave, an MIP-based nanotechnology company, has offered many successful MIP products for the extraction of cannabinoids, which are in the process of commercializing now, and for the detection of COVID-19 [155]. Sixth Wave has also produced MIPs for metal extraction and purification for mining applications.

However, there are bottlenecks in the commercialization of MIPs, with the main one being the production of high-affinity MIPs with a homogeneous size and shape on

a large scale [153]. Failure to ensure homogeneity in terms of the size, shape and affinity reduces the reproducibility of MIPs, which has an undesirable effect on the commercialization of MIPs, but recent improvements in polymer science, methodology and imprinting technology [156–158] has paved the way to ameliorate bottlenecks in the way of commercialization of MT-MIPs. MT-MIPs often require expensive raw materials and complex synthesis methods, which can increase the production costs. To address this, researchers are exploring the use of cheaper monomers and solvents, optimizing the synthesis process to reduce waste, and improving the scalability of production. Additionally, integrating more cost-effective production techniques, such as microfluidic systems, can reduce costs by enabling precise and efficient polymerization processes and improve the stability and reliability for sensor applications. Ensuring the stability of MT-MIPs in various environmental conditions is crucial for their practical application, particularly in sensor technologies. One challenge is the potential degradation of the polymer under harsh conditions (e.g., high temperature or exposure to solvents). To improve the stability, researchers are focusing on enhancing the chemical robustness of the polymers through the selection of appropriate cross-linkers and functional monomers. Additionally, the development of composite materials, such as incorporating MT-MIPs with nanoparticles, can enhance both the mechanical strength and the stability of the sensor. In complex matrices, such as biological or environmental samples, the selectivity and sensitivity of MT-MIP sensors can be compromised due to interference from non-target substances. To mitigate this, the design of MT-MIPs with highly specific binding sites tailored for multiple targets is essential. Optimizing the polymerization process to ensure the formation of high-fidelity binding sites can help improve both selectivity and sensitivity. Moreover, integrating MT-MIPs with microfluidic platforms allows for better control over the interaction between the sensor and the sample, further enhancing the performance [10,25]. Furthermore, practically all the MIP products are currently singleplex MIPs; the production of commercially viable MT-MIPs still has a way to go.

#### 4. Future Perspectives

Molecularly imprinted polymers utilized as artificial receptors have many advantages over natural receptors, making MIPs good recognition elements for sensing applications. The MIP production process is straightforward, and by taking the properties of the targets into consideration, MIPs can be employed for multiplexed detection, which allows the detection of more than one target simultaneously, with many benefits, including saving time and reagents. Electrochemical methods have been preferred to be used in the detection of multiple targets by MT-MIPs because of their significant properties, such as the high sensitivity, simplicity, and fast response. A broad range of targets from amino acids to viruses can be detected by MT-MIP-based electrochemical sensors with high sensitivity and selectivity.

MIPs are preferred over natural receptors because of their high environmental durability, low cost, long shelf life and significant robustness. Despite these advantages, MIPs have some drawbacks, such as the low binding efficiency, challenges in template removal, difficulty in imprinting large molecules, leakage of template, slow rebinding kinetics, cross-selectivity, and sometimes reduced sensitivity [159,160]. All these drawbacks can potentially be addressed by employing appropriate strategies. For example, to overcome the challenges associated with template removal and the imprinting of large molecules, both epitope imprinting [13] and surface imprinting [161] can be utilized. The low binding efficiency can be improved by using MIP nanoparticles, more flexible monomers, and nanomaterials. MIP nanoparticles can enhance the target accessibility, while more flexible polymers can adapt to slight conformational changes.

The recognition efficiency of MIPs can be further enhanced by employing surface imprinting, nanoparticles, microfluidic systems, and hybrid recognition strategies that incorporate highly specific aptamers with MIPs. Aptamers are nucleic acid sequences (single-stranded DNA or RNA) that can be recognized and bound to their target molecule. Aptamers offer great benefits, including being chemically stable, easily modified chemically and easily synthesized, which can increase the sensitivity and selectivity. Because of the unique properties of both aptamers and MIPs, they have been used as a hybrid recognition element for the detection of many substances [162–165]. MIPs are more stable against pH, temperature changes and organic solvents than aptamers and aptamers are more selective than MIPs. By combining MIPs and aptamers, the selectivity and sensitivity can be enhanced, and increased stability and high binding affinity can be obtained [159].

Template leakage is another common limitation of MIPs. To eliminate or alleviate this issue, dummy templates, structural analogues of the target molecules, can be used [166]. After polymerization, UV or plasma treatments can be applied to degrade residual templates. Buried binding sites within the polymer may slow the diffusion of target molecules. This limitation can be overcome by using surface imprinting and nanomaterials to create accessible binding sites, thereby increasing the surface area and enhancing the binding rates. Additionally, utilizing highly selective functional monomers that interact only with unique functional groups of the template, along with hybrid MIPs, can help reduce the effect of cross-reactivity.

In MT-MIPs, the analyte may sometimes contain multiple recognizable substances simultaneously. For example, if two templates have the same oxidation potentials, it can make the specific recognition of the templates challenging. In such cases, a “surface grafting” approach can be used to distinguish and detect specific targets [82]. For non-electroactive templates, introducing electroactive labels specific to each analyte can be another strategy for distinguishing multiple recognizable substances. Each label can produce a distinct, recognizable electrochemical signal.

So far, many MIPs and MT-MIPs have been produced for sensing applications targeting various analytes, including both electroactive and non-electroactive targets. Electroactive targets, such as inorganic ions, certain pharmaceuticals (including paracetamol and epinephrine), and environmental pollutants (such as phenol), have been detected using MIPs and MT-MIPs [167–169]. Non-electroactive targets, including proteins such as prostate-specific antigen (PSA), lipids, and bacteria, have also been detected by MIPs and MT-MIPs. For example, Tamboli et al. constructed a MOSFET device to detect PSA in human plasma by using a hybrid synthetic receptor consisting of an MIP and a PSA-specific aptamer [170]. In this study, the aptamer-coupled MIP was immobilized on a gold electrode, and the response generated as a result of binding was converted into an electrical signal by a field-effect transistor. The sensor performance was analyzed by exposing the sensor to different PSA concentrations and measuring the resulting voltage changes corresponding to those concentrations. In another study, Agar et al. developed an electrochemical sensor utilizing aptamers and MIPs as recognition elements for the multiplexed detection of *Escherichia coli* (*E. coli*) and *Staphylococcus aureus* (*S. aureus*) [171]. After preparing two different sensors—one for *E. coli* and the other for *S. aureus*—both sensors were transferred onto the same electrode array to conduct multiplexed detection of both bacteria. Non-Faradaic electrochemical impedance spectroscopy (EIS) measurements were employed to evaluate the sensor response.

The application of MT-MIPs and MIPs on complex matrices faces several challenges, such as matrix interference, cross-reactivity and limited accessibility. In terms of the matrix interference effect, non-target components in the sample matrix can occupy recognition sites or interfere with detection signals, reducing the specificity and sensitivity. Co-existing

molecules structurally similar to templates may bind to the recognition sites and cause cross-reactivity. The complex nature of real samples can hinder target molecules from accessing recognition sites effectively, inducing limited accessibility. To overcome these challenges, several methods can be introduced. Designing MT-MIPs or MIPs with surface binding sites can improve the accessibility for target molecules and reduce non-specific binding. Sample pre-treatments such as filtration [172], centrifugation [173] or dilution can eliminate unwanted matrix components. Using hybrid materials such as magnetic nanoparticles or graphene oxide can enhance separation from complex samples and reduce interference. In the study conducted by Nurrokhimah et al., Fe<sub>3</sub>O<sub>4</sub>@SiO<sub>2</sub>-based magnetic multi-template molecularly imprinted polymers (MT-MIPs) were developed for simultaneous detection of antibiotics (cephalexin, cefazolin, and cefoperazone) in milk [23]. The synthesis involved a composite material to improve the extraction efficiency and reduce the matrix interference. Pre-treatment processes, like centrifugation and filtration, were used to reduce milk's complex matrix interference, while washing steps optimized the removal of non-specific binding.

Considering the advantages provided by the design of microfluidic systems, their integration with MT-MIP-based electrochemical sensors for multiplexed detection is encouraging. Many companies that previously produced MIPs for purification and separation applications can produce MIPs that can be used for multiplexed detection by eliminating some of the problems that prevent MIPs from being produced on a large scale, and thus MT-MIPs may become available as POC diagnostic tools in the near future.

MIPs are very promising artificial receptors that can replace natural recognition elements. MT-MIP sensors provide the ability to measure different analytes on the same sample. The MIPs' capability of detecting a broad range of targets, incorporation with other recognition elements, integration of microfluidics and easy preparation process allow them to be used for multiplexed detection of different targets.

**Author Contributions:** Conceptualization, M.A.; investigation, M.A.; writing—original draft preparation, M.A.; writing—review and editing, M.L., H.S.L. and P.E.; supervision, M.L., H.S.L. and P.E. All authors have read and agreed to the published version of the manuscript.

**Funding:** M.A. was funded by the Ministry of National Education of Türkiye through their YLSY International Graduate Education Scholarship program.

**Institutional Review Board Statement:** Not applicable

**Informed Consent Statement:** Not applicable

**Data Availability Statement:** Not applicable

**Conflicts of Interest:** The authors declare no conflicts of interest.

## References

1. Aydin, E.B.; Aydin, M.; Sezginturk, M.K. Biosensors in Drug Discovery and Drug Analysis. *Curr. Anal. Chem.* **2019**, *15*, 467–484. [[CrossRef](#)]
2. Abu, H.; Hossain, M.A.M.; Marlinda, A.; Al Mamun, M.; Simarani, K.; Johan, M.R. Nanomaterials Based Electrochemical Nucleic Acid Biosensors for Environmental Monitoring: A Review. *Appl. Surf. Sci. Adv.* **2021**, *4*, 100064. [[CrossRef](#)]
3. Chaudhry, G.E.S.; Akim, A.M.; Safdar, N.; Yasmin, A.; Begum, S.; Sung, Y.Y.; Sifzizul, T.; Muhammad, T. Cancer and Disease Diagnosis-Biosensor as Potential Diagnostic Tool for Biomarker Detection. *J. Adv. Pharm. Technol. Res.* **2022**, *13*, 243–247. [[CrossRef](#)] [[PubMed](#)]
4. Mi, F.; Hu, C.M.; Wang, Y.; Wang, L.; Peng, F.; Geng, P.F.; Guan, M. Recent Advancements in Microfluidic Chip Biosensor Detection of Foodborne Pathogenic Bacteria: A Review. *Anal. Bioanal. Chem.* **2022**, *414*, 2883–2902. [[CrossRef](#)] [[PubMed](#)]
5. Chen, Z.L.; Xie, M.J.; Zhao, F.G.; Han, S.Y. Application of Nanomaterial Modified Aptamer-Based Electrochemical Sensor in Detection of Heavy Metal Ions. *Foods* **2022**, *11*, 1404. [[CrossRef](#)] [[PubMed](#)]

6. Naresh, V.; Lee, N. A Review on Biosensors and Recent Development of Nanostructured Materials-Enabled Biosensors. *Sensors* **2021**, *21*, 1109. [[CrossRef](#)]
7. Sajini, T.; Mathew, B. A Brief Overview of Molecularly Imprinted Polymers: Highlighting Computational Design, Nano and Photo-Responsive Imprinting. *Talanta Open* **2021**, *4*, 20. [[CrossRef](#)]
8. Refaat, D.; Aggour, M.; Farghali, A.; Mahajan, R.; Wiklander, J.; Nicholls, I.; Piletsky, S. Strategies for Molecular Imprinting and the Evolution of MIP Nanoparticles as Plastic Antibodies-Synthesis and Applications. *Int. J. Mol. Sci.* **2019**, *20*, 6304. [[CrossRef](#)] [[PubMed](#)]
9. Wackerlig, J.; Lieberzeit, P.A. Molecularly Imprinted Polymer Nanoparticles in Chemical Sensing—Synthesis, Characterisation and Application. *Sens. Actuators B-Chem.* **2015**, *207*, 144–157. [[CrossRef](#)]
10. Hasanah, A.N.; Safitri, N.; Zulfa, A.; Neli, N.; Rahayu, D. Factors Affecting Preparation of Molecularly Imprinted Polymer and Methods on Finding Template-Monomer Interaction as the Key of Selective Properties of the Materials. *Molecules* **2021**, *26*, 5612. [[CrossRef](#)] [[PubMed](#)]
11. Chen, L.X.; Wang, X.Y.; Lu, W.H.; Wu, X.Q.; Li, J.H. Molecular Imprinting: Perspectives and Applications. *Chem. Soc. Rev.* **2016**, *45*, 2137–2211. [[CrossRef](#)]
12. Kodakat, K.; Kumar, K.G. Fabrication of a Selective and Sensitive Electro-synthesized Molecularly Imprinted Polymer-based Electrochemical Sensor for the Determination of Xanthine. *J. Appl. Electrochem.* **2023**, *53*, 2259–2272. [[CrossRef](#)]
13. Gupta, N.; Shah, K.; Singh, M. An Epitope-Imprinted Piezoelectric Diagnostic Tool for *Neisseria meningitidis* detection. *J. Mol. Recognit.* **2016**, *29*, 572–579. [[CrossRef](#)] [[PubMed](#)]
14. Wang, Y.L.; Gao, Y.L.; Wang, P.P.; Shang, H.; Pan, S.Y.; Li, X.J. Sol-gel Molecularly Imprinted Polymer for Selective Solid Phase Microextraction of Organophosphorous Pesticides. *Talanta* **2013**, *115*, 920–927. [[CrossRef](#)] [[PubMed](#)]
15. Lah, N.F.C.; Ahmad, A.L.; Low, S.C.; Zaulkiflee, N.D. Isotherm and Electrochemical Properties of Atrazine Sensing Using PVC/MIP: Effect of Porogenic Solvent Concentration Ratio. *Membranes* **2021**, *11*, 657. [[CrossRef](#)]
16. Wang, S.; Zhang, L.; Zeng, J.; Hu, X.; Wang, X.; Yu, L.; Wang, D.; Cheng, L.; Ahmed, R.; Romanovski, V.; et al. Multi-templates Molecularly Imprinted Polymers for Simultaneous Recognition of Multiple Targets: From Academy to Application. *Trac-Trends Anal. Chem.* **2023**, *166*, 117173. [[CrossRef](#)]
17. Nishimura, K.; Okamura, N.; Kimachi, T.; Haginaka, J. Evaluation of Molecularly Imprinted Polymers for Chlorpromazine and Bromopromazine Prepared by Multi-step Swelling and Polymerization Method-The Application for the Determination of Chlorpromazine and Its Metabolites in Rat Plasma by Column-switching LC. *J. Pharm. Biomed. Anal.* **2019**, *174*, 248–255. [[CrossRef](#)]
18. Sun, C.; Wang, J.; Huang, J.; Yao, D.; Wang, C.; Zhang, L.; Hou, S.; Chen, L.; Yuan, C. The Multi-Template Molecularly Imprinted Polymer Based on SBA-15 for Selective Separation and Determination of *Panax notoginseng* Saponins Simultaneously in Biological Samples. *Polymers* **2017**, *9*, 653. [[CrossRef](#)]
19. Ji, W.; Xie, H.; Zhou, J.; Wang, X.; Ma, X.; Huang, L. Water-compatible Molecularly Imprinted Polymers for Selective Solid Phase Extraction of Dencichine from the Aqueous Extract of *Panax notoginseng*. *J. Chromatogr. B-Anal. Technol. Biomed. Life Sci.* **2016**, *1008*, 225–233. [[CrossRef](#)] [[PubMed](#)]
20. Nkosi, S.; Mahlambi, P.; Chimuka, L. Synthesis, Characterisation and Optimisation of Bulk Molecularly Imprinted Polymers from Nonsteroidal Anti-inflammatory Drugs. *S. Afr. J. Chem.-Suid-Afr. Tydskr. Vir Chem.* **2022**, *76*, 56–64. [[CrossRef](#)]
21. Miura, C.; Funaya, N.; Matsunaga, H.; Haginaka, J. Monodisperse, Molecularly Imprinted Polymers for Creatinine by Modified Precipitation Polymerization and Their Applications to Creatinine Assays for Human Serum and Urine. *J. Pharm. Biomed. Anal.* **2013**, *85*, 288–294. [[CrossRef](#)]
22. Wu, X.; Shimizu, K. Development of Molecularly Imprinted Polymers as Tailored Templates for the Solid-state [2+2] photodimerization. *Biosens. Bioelectron.* **2009**, *25*, 640–646. [[CrossRef](#)]
23. Nurrokhimah, M.; Nurerk, P.; Kanatharana, P.; Bunkoed, O. A Nanosorbent Consisting of a Magnetic Molecularly Imprinted Polymer and Graphene Oxide for Multi-residue Analysis of Cephalosporins. *Microchim. Acta* **2019**, *186*, 822. [[CrossRef](#)] [[PubMed](#)]
24. Pratama, K.F.; Manik, M.E.R.; Rahayu, D.; Hasanah, A.N. Effect of the Molecularly Imprinted Polymer Component Ratio on Analytical Performance. *Chem. Pharm. Bull.* **2020**, *68*, 1013–1024. [[CrossRef](#)] [[PubMed](#)]
25. Murdaya, N.; Triadenda, A.L.; Rahayu, D.; Hasanah, A.N. A Review: Using Multiple Templates for Molecular Imprinted Polymer: Is It Good? *Polymers* **2022**, *14*, 4441. [[CrossRef](#)] [[PubMed](#)]
26. Xu, R.; Tian, J.; Guan, Y.; Zhang, Y. Peptide-Cross-Linked Protein-Imprinted Polymers: Easy Template Removal and Excellent Imprinting Effect. *CCS Chem.* **2019**, *1*, 544–552. [[CrossRef](#)]
27. Ge, Y.; Turner, A. Too Large to Fit? Recent Developments in Macromolecular Imprinting. *Trends Biotechnol.* **2008**, *26*, 218–224. [[CrossRef](#)]
28. Fatma, S.; Prasad, B.B.; Singh, K.; Singh, R.; Jaiswal, S. A Reduced Graphene Oxide Ceramic Electrode Modified with One MoNomer Doubly Imprinted Acryloylated Tetraamine Cobalt Phthalocyanine Polymer for the Simultaneous Analysis of Anti-cancerous Drugs. *Sens. Actuators. B Chem.* **2019**, *281*, 139–149. [[CrossRef](#)]



29. Bali Prasad, B.; Jauhari, D.; Prasad Tiwari, M. A Dual-template Imprinted Polymer-modified Carbon Ceramic Electrode for Ultra Trace Simultaneous Analysis of Ascorbic Acid and Dopamine. *Biosens. Bioelectron.* **2013**, *50*, 19–27. [[CrossRef](#)]
30. Prasad, B.B.; Jauhari, D.; Tiwari, M.P. Doubly Imprinted Polymer Nanofilm-modified Electrochemical Sensor for Ultra-trace Simultaneous Analysis of Glyphosate and Glufosinate. *Biosens. Bioelectron.* **2014**, *59*, 81–88. [[CrossRef](#)] [[PubMed](#)]
31. Prasad, B.; Pathak, P. Development of Surface Imprinted Nanospheres Using the Inverse Suspension Polymerization Method for Electrochemical Ultra Sensing of Dacarbazine. *Anal. Chim. Acta* **2017**, *974*, 75–86. [[CrossRef](#)]
32. Tang, K.L.; Chen, Y.; Wang, X.N.; Zhou, Q.; Lei, H.B.; Yang, Z.X.; Zhang, Z.H. Smartphone-integrated Tri-color Fluorescence Sensing Platform Based on Acid-sensitive Fluorescence Imprinted Polymers for Dual-mode Visual Intelligent Detection of Ibuprofen, Chloramphenicol and Florfenicol. *Anal. Chim. Acta* **2023**, *1260*, 341174. [[CrossRef](#)] [[PubMed](#)]
33. Zhu, L.; Mei, X.C.; Peng, Z.C.; Yang, J.; Li, Y.C. A Paper-based Microfluidic Sensor Array Combining Molecular Imprinting Technology and Carbon Quantum Dots for the Discrimination of Nitrophenol Isomers. *J. Hazard. Mater.* **2022**, *435*, 129012. [[CrossRef](#)]
34. Wang, L.Y.; Li, B.W.; Wang, J.A.; Qi, J.; Li, J.H.; Ma, J.P.; Chen, L.X. A Rotary Multi-positioned Cloth/Paper Hybrid Microfluidic Device for Simultaneous Fluorescence Sensing of Mercury and Lead Ions by Using Ion Imprinted Technologies. *J. Hazard. Mater.* **2022**, *428*, 128165. [[CrossRef](#)] [[PubMed](#)]
35. Feng, F.; Zheng, J.W.; Qin, P.; Han, T.; Zhao, D.Y. A Novel Quartz Crystal Microbalance Sensor Array Based on Molecular Imprinted Polymers for Simultaneous Detection of Clenbuterol and Its Metabolites. *Talanta* **2017**, *167*, 94–102. [[CrossRef](#)] [[PubMed](#)]
36. Liu, N.; Li, X.L.; Ma, X.H.; Ou, G.R.; Gao, Z.X. Rapid and Multiple Detections of Staphylococcal Enterotoxins by Two-dimensional Molecularly Imprinted Film-coated QCM Sensor. *Sens. Actuators B-Chem.* **2014**, *191*, 326–331. [[CrossRef](#)]
37. Cai, Y.; He, X.; Cui, P.L.; Liu, J.; Li, Z.B.; Jia, B.J.; Zhang, T.; Wang, J.P.; Yuan, W.Z. Preparation of a Chemiluminescence Sensor for Multi-detection of Benzimidazoles in Meat Based on Molecularly Imprinted Polymer. *Food Chem.* **2019**, *280*, 103–109. [[CrossRef](#)] [[PubMed](#)]
38. Zhang, T.; Liu, J.; Wang, J.P. Preparation of a Molecularly Imprinted Polymer Based Chemiluminescence Sensor for the Determination of Amantadine and Rimantadine in Meat. *Anal. Methods* **2018**, *10*, 5025–5031. [[CrossRef](#)]
39. Haginaka, J.; Tabo, H.; Matsunaga, H. Preparation of Molecularly Imprinted Polymers for Organophosphates and Their Application to the Recognition of Organophosphorus Compounds and Phosphopeptides. *Anal. Chim. Acta* **2012**, *748*, 1–8. [[CrossRef](#)]
40. Yan, M.M.; She, Y.X.; Cao, X.L.; Ma, J.; Chen, G.; Hong, S.H.; Shao, Y.; Abd El-Aty, A.M.; Wang, M.; Wang, J. A Molecularly Imprinted Polymer with Integrated Gold Nanoparticles for Surface Enhanced Raman Scattering Based Detection of the Triazine Herbicides, Prometryn and Simetryn. *Microchim. Acta* **2019**, *186*, 143. [[CrossRef](#)] [[PubMed](#)]
41. Lu, Z.; Li, Y.; Liu, T.; Wang, G.; Sun, M.; Jiang, Y.; He, H.; Wang, Y.; Zou, P.; Wang, X.; et al. A Dual-Template Imprinted Polymer Electrochemical Sensor Based on AuNPs and Nitrogen-doped Graphene Oxide Quantum Dots Coated on NiS<sub>2</sub>/Biomass Carbon for Simultaneous Determination of Dopamine and Chlorpromazine. *Chem. Eng. J.* **2020**, *389*, 124417. [[CrossRef](#)]
42. Siavash Moakhar, R.; del Real Mata, C.; Jalali, M.; Shafique, H.; Sanati, A.; Vries, J.; Strauss, J.; AbdElFatah, T.; Ghasemi, F.; McLean, M.; et al. A Versatile Biomimic Nanotemplating Fluidic Assay for Multiplex Quantitative Monitoring of Viral Respiratory Infections and Immune Responses in Saliva and Blood. *Adv. Sci.* **2022**, *9*, 2204246. [[CrossRef](#)] [[PubMed](#)]
43. Wang, L.; Zhang, W. Molecularly Imprinted Polymer (MIP) Based Electrochemical Sensors and Their Recent Advances in Health Applications. *Sens. Actuators Rep.* **2023**, *5*, 100153. [[CrossRef](#)]
44. Ostojic, J.; Herenda, S.; Besic, Z.; Milos, M.; Galic, B. Advantages of an Electrochemical Method Compared to the Spectrophotometric Kinetic Study of Peroxidase Inhibition by Boroxine Derivative. *Molecules* **2017**, *22*, 1120. [[CrossRef](#)] [[PubMed](#)]
45. Kusumkar, V.V.; Galambos, M.; Viglasova, E.; Dano, M.; Smelkova, J. Ion-Imprinted Polymers: Synthesis, Characterization, and Adsorption of Radionuclides. *Materials* **2021**, *14*, 1083. [[CrossRef](#)] [[PubMed](#)]
46. Fu, J.Q.; Chen, L.X.; Li, J.H.; Zhang, Z. Current Status and Challenges of Ion Imprinting. *J. Mater. Chem. A* **2015**, *3*, 13598–13627. [[CrossRef](#)]
47. Bali Prasad, B.; Jauhari, D.; Verma, A. A Dual-Ion Imprinted Polymer Embedded in Sol–Gel Matrix for the Ultra Trace Simultaneous Analysis of Cadmium and Copper. *Talanta* **2014**, *120*, 398–407. [[CrossRef](#)] [[PubMed](#)]
48. Behbahani, M.; Barati, M.; Bojdi, M.K.; Pourali, A.R.; Bagheri, A.; Tapeh, N.A.G. A Nanosized Cadmium(II)-Imprinted Polymer for Use in Selective Trace Determination of Cadmium in Complex Matrices. *Microchim. Acta* **2013**, *180*, 1117–1125. [[CrossRef](#)]
49. Shamsipur, M.; Fasihi, J.; Khanchi, A.; Hassani, R.; Alizadeh, K.; Shamsipur, H. A Stoichiometric Imprinted Chelating Resin for Selective Recognition of Copper(II) Ions in Aqueous Media. *Anal. Chim. Acta* **2007**, *599*, 294–301. [[CrossRef](#)] [[PubMed](#)]
50. Birlik, E.; Ersöz, A.; Denizli, A.; Say, R. Preconcentration of Copper Using Double-Imprinted Polymer via Solid Phase Extraction. *Anal. Chim. Acta* **2006**, *565*, 145–151. [[CrossRef](#)]
51. Prasad, B.B.; Jauhari, D. Double-ion Imprinted Polymer @Magnetic Nanoparticles Modified Screen Printed Carbon Electrode for Simultaneous Analysis of Cerium and Gadolinium Ions. *Anal. Chim. Acta* **2015**, *875*, 83–91. [[CrossRef](#)] [[PubMed](#)]

52. Karim, M.M.; Lee, S.H.; Kim, Y.S.; Bae, H.S.; Hong, S.B. Fluorimetric Determination of Cerium(IV) with Ascorbic Acid. *J. Fluoresc.* **2006**, *16*, 17–22. [[CrossRef](#)] [[PubMed](#)]
53. Focarelli, F.; Giachino, A.; Waldron, K.J. Copper Microenvironments in the Human Body Define Patterns of Copper Adaptation in Pathogenic Bacteria. *PLoS Pathog.* **2022**, *18*, e1010617. [[CrossRef](#)] [[PubMed](#)]
54. Chasapis, C.T.; Loutsidou, A.C.; Spiliopoulou, C.A.; Stefanidou, M.E. Zinc and Human Health: An Update. *Arch. Toxicol.* **2012**, *86*, 521–534. [[CrossRef](#)] [[PubMed](#)]
55. Wilschefski, S.C.; Baxter, M.R. Inductively Coupled Plasma Mass Spectrometry: Introduction to Analytical Aspects. *Clin. Biochem. Rev.* **2019**, *40*, 115–133. [[CrossRef](#)]
56. Kumar, D.; Madhuri, R.; Prasad Tiwari, M.; Sinha, P.; Bali Prasad, B. Molecularly Imprinted Polymer-Modified Electrochemical Sensor for Simultaneous Determination of Copper and Zinc. *Adv. Mater. Lett.* **2011**, *2*, 294–297. [[CrossRef](#)]
57. Lv, Y.Q.; Tan, T.W.; Svec, F. Molecular Imprinting of Proteins in Polymers Attached to The Surface of Nanomaterials for Selective Recognition of Biomacromolecules. *Biotechnol. Adv.* **2013**, *31*, 1172–1186. [[CrossRef](#)] [[PubMed](#)]
58. Dinc, M.; Esen, C.; Mizaikoff, B. Recent Advances on Core-Shell Magnetic Molecularly Imprinted Polymers for Biomacromolecules. *Trac-Trends Anal. Chem.* **2019**, *114*, 202–217. [[CrossRef](#)]
59. Mazzotta, E.; Di Giulio, T.; Malitesta, C. Electrochemical Sensing of Macromolecules Based on Molecularly Imprinted Polymers: Challenges, Successful Strategies, and Opportunities. *Anal. Bioanal. Chem.* **2022**, *414*, 5165–5200. [[CrossRef](#)]
60. El-Schich, Z.; Zhang, Y.; Feith, M.; Beyer, S.; Sternbæk, L.; Ohlsson, L.; Stollenwerk, M.; Wingren, A.G. Molecularly Imprinted Polymers in Biological Applications. *Biotechniques* **2020**, *69*, 406–419. [[CrossRef](#)] [[PubMed](#)]
61. Song, Q.M.; Wang, B.W.; Lv, Y.Q. Molecularly imprinted monoliths: Recent Advances in the Selective Recognition of Biomacromolecules Related Biomarkers. *J. Sep. Sci.* **2022**, *45*, 1469–1481. [[CrossRef](#)]
62. Nontawong, N.; Ngao Sri, P.; Chunta, S.; Jarujamrus, P.; Nacapricha, D.; Lieberzeit, P.A.; Amatatongchai, M. Smart Sensor for Assessment of Oxidative/Nitrative Stress Biomarkers Using A Dual-Imprinted Electrochemical Paper-Based Analytical Device. *Anal. Chim. Acta* **2022**, *1191*, 339363. [[CrossRef](#)] [[PubMed](#)]
63. Martins, G.V.; Tavares, A.P.M.; Fortunato, E.; Sales, M.G.F. Paper-Based Sensing Device for Electrochemical Detection of Oxidative Stress Biomarker 8-Hydroxy-2'-deoxyguanosine (8-OHdG) in Point-of-Care. *Sci. Rep.* **2017**, *7*, 14558. [[CrossRef](#)]
64. Wang, S.Q.; Sun, G.H.; Chen, Z.G.; Liang, Y.W.; Zhou, Q.; Pan, Y.F.; Zhai, H.Y. Constructing a Novel Composite of Molecularly Imprinted Polymer-Coated AuNPs Electrochemical Sensor for the Determination of 3-Nitrotyrosine. *Electrochim. Acta* **2018**, *259*, 893–902. [[CrossRef](#)]
65. Jia, L.P.; Wang, H.S. Electrochemical Reduction Synthesis of Graphene/Nafion Nanocomposite Film and Its Performance on the Detection of 8-Hydroxy-2'-Deoxyguanosine in the Presence of Uric Acid. *J. Electroanal. Chem.* **2013**, *705*, 37–43. [[CrossRef](#)]
66. Luo, K.; Zhao, C.; Luo, Y.; Pan, C.; Li, J. Electrochemical Sensor for the Simultaneous Detection of CA72-4 And CA19-9 Tumor Markers Using Dual Recognition via Glycosyl Imprinting and Lectin-Specific Binding for Accurate Diagnosis of Gastric Cancer. *Biosens. Bioelectron.* **2022**, *216*, 114672. [[CrossRef](#)] [[PubMed](#)]
67. Hong, G.L.; Chen, R.T.; Xu, L.Y.; Lu, X.; Yang, Z.Q.; Zhou, G.B.; Li, L.; Chen, W.; Peng, H.P. One-pot Ultrasonic Synthesis of Multifunctional Au Nanoparticle-Ferrocene-WS<sub>2</sub> Nanosheet Composite for the Construction of an Electrochemical Biosensing Platform. *Anal. Chim. Acta* **2020**, *1099*, 52–59. [[CrossRef](#)] [[PubMed](#)]
68. Wang, R.; Feng, J.J.; Liu, W.D.; Jiang, L.Y.; Wang, A.J. A Novel Label-Free Electrochemical Immunosensor Based on the Enhanced Catalytic Currents of Oxygen Reduction by AuAg Hollow Nanocrystals for Detecting Carbohydrate Antigen 199. *Biosens. Bioelectron.* **2017**, *96*, 152–158. [[CrossRef](#)]
69. Wang, D.; Gan, N.; Zhang, H.; Li, T.; Qiao, L.; Cao, Y.; Su, X.; Jiang, S. Simultaneous Electrochemical Immunoassay Using Graphene–Au Grafted Recombinant Apoferritin-Encoded Metallic Labels As Signal Tags and Dual-Template Magnetic Molecular Imprinted Polymer As Capture Probes. *Biosens. Bioelectron.* **2015**, *65*, 78–82. [[CrossRef](#)] [[PubMed](#)]
70. Kong, F.Y.; Xu, B.Y.; Xu, J.J.; Chen, H.Y. Simultaneous Electrochemical Immunoassay Using Cds/DNA and Pbs/DNA Nanochains As Labels. *Biosens. Bioelectron.* **2013**, *39*, 177–182. [[CrossRef](#)] [[PubMed](#)]
71. Taheri, N.; Khoshshafar, H.; Ghanei, M.; Ghazvini, A.; Bagheri, H. Dual-template Rectangular Nanotube Molecularly Imprinted Polypyrrole for Label-Free Impedimetric Sensing of AFP and CEA As Lung Cancer Biomarkers. *Talanta* **2022**, *239*, 123146. [[CrossRef](#)]
72. Zhao, X.Q.; Wang, J.; Chen, H.; Xu, H.; Bai, L.J.; Wang, W.X.; Yang, H.W.; Wei, D.L.; Yuan, B.Q. A Multiple Signal Amplification Based on PEI and rGO Nanocomposite for Simultaneous Multiple Electrochemical Immunoassay. *Sens. Actuators B-Chem.* **2019**, *301*, 127071. [[CrossRef](#)]
73. Li, L.H.; Wei, Y.; Zhang, S.P.; Chen, X.S.; Shao, T.L.; Feng, D.X. Electrochemical Immunosensor Based on Metal Ions Functionalized CNSs@Au NPs Nanocomposites As Signal Amplifier for Simultaneous Detection of Triple Tumor Markers. *J. Electroanal. Chem.* **2021**, *880*, 114882. [[CrossRef](#)]

74. Karami, P.; Bagheri, H.; Johari-Ahar, M.; Khoshsafar, H.; Arduini, F.; Afkhami, A. Dual-modality Impedimetric Immunosensor for Early Detection of Prostate-Specific Antigen and Myoglobin Markers Based on Antibody-Molecularly Imprinted Polymer. *Talanta* **2019**, *202*, 111–122. [[CrossRef](#)]
75. Merriel, S.W.D.; Pocock, L.; Gilbert, E.; Creavin, S.; Walter, F.M.; Spencer, A.; Hamilton, W. Systematic Review and Meta-Analysis of the Diagnostic Accuracy of Prostate-Specific Antigen (PSA) for the Detection of Prostate Cancer in Symptomatic Patients. *BMC Med.* **2022**, *20*, 54. [[CrossRef](#)] [[PubMed](#)]
76. Johari-Ahar, M.; Karami, P.; Ghanei, M.; Afkhami, A.; Bagheri, H. Development of a Molecularly Imprinted Polymer Tailored on Disposable Screen-Printed Electrodes for Dual Detection of EGFR and VEGF Using Nano-Liposomal Amplification Strategy. *Biosens. Bioelectron.* **2018**, *107*, 26–33. [[CrossRef](#)]
77. Li, R.B.; Huang, H.M.; Huang, L.Z.; Lin, Z.Y.; Guo, L.H.; Qiu, B.; Chen, G.N. Electrochemical Biosensor for Epidermal Growth Factor Receptor Detection with Peptide Ligand. *Electrochim. Acta* **2013**, *109*, 233–237. [[CrossRef](#)]
78. Omidfar, K.; Darzianiazizi, M.; Ahmadi, A.; Daneshpour, M.; Shirazi, H. A High Sensitive Electrochemical Nanoimmunosensor Based on Fe<sub>3</sub>O<sub>4</sub>/TMC/Au Nanocomposite and PT-Modified Electrode for the Detection of Cancer Biomarker Epidermal Growth Factor Receptor. *Sens. Actuators B-Chem.* **2015**, *220*, 1311–1319. [[CrossRef](#)]
79. Nonaka, Y.; Abe, K.; Ikebukuro, K. Electrochemical Detection of Vascular Endothelial Growth Factor with Aptamer Sandwich. *Electrochemistry* **2012**, *80*, 363–366. [[CrossRef](#)]
80. Pandey, I.; Tiwari, J.D. A Novel Dual Imprinted Conducting Nanocubes Based Flexible Sensor for Simultaneous Detection of Hemoglobin and Glycated Haemoglobin in Gestational Diabetes Mellitus Patients. *Sens. Actuators. B Chem.* **2019**, *285*, 470–478. [[CrossRef](#)]
81. Liu, Z.; Yin, Z.-Z.; Zheng, G.; Zhang, H.; Zhou, M.; Li, S.; Kong, Y. Dual-template Molecularly Imprinted Electrochemical Biosensor for IgG-IgM Combined Assay Based on a Dual-Signal Strategy. *Bioelectrochemistry* **2022**, *148*, 108267. [[CrossRef](#)] [[PubMed](#)]
82. Prasad, B.B.; Jaiswal, S.; Singh, K. Ultra-trace Analysis of D-And L-Aspartic Acid Applying One-By-One Approach on a Dual Imprinted Electrochemical Sensor. *Sens. Actuators. B Chem.* **2017**, *240*, 631–639. [[CrossRef](#)]
83. Hou, H.; Tang, S.; Wang, W.; Liu, M.; Liang, A.; Sun, L.; Luo, A. Electrochemical Enantioanalysis of D-and L-Cysteine with a Dual-Template Molecularly Imprinted Sensor. *J. Electrochem. Soc.* **2022**, *169*, 037506. [[CrossRef](#)]
84. Zaidi, S.A. Facile and Efficient Electrochemical Enantiomer Recognition of Phenylalanine Using B-Cyclodextrin Immobilized on Reduced Graphene Oxide. *Biosens. Bioelectron.* **2017**, *94*, 714–718. [[CrossRef](#)]
85. Yang, X.; Niu, X.H.; Mo, Z.L.; Wang, J.; Shuai, C.; Pan, Z.; Liu, Z.Y.; Liu, N.J.; Guo, R.B. 3D Nitrogen and Sulfur Co -Doped Graphene/Integrated Polysaccharides for Electrochemical Recognition Tryptophan Enantiomers. *J. Electrochem. Soc.* **2019**, *166*, B1053–B1062. [[CrossRef](#)]
86. Afsharara, H.; Asadian, E.; Mosta, B.; Banan, K.; Bigdeli, S.A.; Hatamabadi, D.; Keshavarz, A.; Hussain, C.M.; Kecili, R.; Ghorbani-Bidkorpheh, F. Molecularly Imprinted Polymer-Modified Carbon Paste Electrodes (MIP-CPE): A Review on Sensitive Electrochemical Sensors for Pharmaceutical Determinations. *Trac-Trends Anal. Chem.* **2023**, *160*, 116949. [[CrossRef](#)]
87. Ramanavicius, S.; Samukaite-Bubniene, U.; Ratautaite, V.; Bechelany, M.; Ramanavicius, A. Electrochemical Molecularly Imprinted Polymer Based Sensors for Pharmaceutical and Biomedical Applications (Review). *J. Pharm. Biomed. Anal.* **2022**, *215*, 114739. [[CrossRef](#)]
88. Singh, R.; Singh, M. Design of Imprinting Matrix for Dual Template Sensing via Electropolymerized Polythiophene Films. *J. Mol. Recognit.* **2022**, *35*, e2962. [[CrossRef](#)]
89. Mulik, B.B.; Dhupal, S.T.; Sapner, V.S.; Rehman, N.; Dixit, P.P.; Sathe, B.R. Graphene Oxide-Based Electrochemical Activation of Ethionamide Towards Enhanced Biological Activity. *Rsc Adv.* **2019**, *9*, 35463–35472. [[CrossRef](#)] [[PubMed](#)]
90. Kushwaha, A.; Singh, S.; Gupta, N.; Singh, A.K.; Singh, M. Synthesis and Characterization of Antipyrine-Imprinted Polymers and Their Application for Sustained Release. *Polym. Bull.* **2018**, *75*, 5235–5252. [[CrossRef](#)]
91. Sun, Y.; He, J.; Waterhouse, G.I.N.; Xu, L.; Zhang, H.; Qiao, X.; Xu, Z. A Selective Molecularly Imprinted Electrochemical Sensor With GO@COF Signal Amplification for the Simultaneous Determination of Sulfadiazine and Acetaminophen. *Sens. Actuators. B Chem.* **2019**, *300*, 126993. [[CrossRef](#)]
92. Teleanu, R.I.; Niculescu, A.G.; Roza, E.; Vladăncenco, O.; Grumezescu, A.M.; Teleanu, D.M. Neurotransmitters-Key Factors in Neurological and Neurodegenerative Disorders of the Central Nervous System. *Int. J. Mol. Sci.* **2022**, *23*, 5954. [[CrossRef](#)] [[PubMed](#)]
93. Si, B.; Song, E. Recent Advances in the Detection of Neurotransmitters. *Chemosensors* **2018**, *6*, 1. [[CrossRef](#)]
94. Si, B.; Song, E. Molecularly Imprinted Polymers for the Selective Detection of Multi-Analyte Neurotransmitters. *Microelectron. Eng.* **2018**, *187–188*, 58–65. [[CrossRef](#)]
95. Liu, W.; Cui, F.; Li, H.; Wang, S.; Zhuo, B. Three-dimensional Hybrid Networks of Molecularly Imprinted Poly(9-Carbazoleacetic Acid) and MWCNTs for Simultaneous Voltammetric Determination of Dopamine and Epinephrine in Plasma Sample. *Sens. Actuators. B Chem.* **2020**, *323*, 128669. [[CrossRef](#)]

96. Fatma, S.; Prasad, B.B.; Jaiswal, S.; Singh, R.; Singh, K. Electrochemical Simultaneous Analysis of Dopamine and Epinephrine Using Double Imprinted One Monomer Acryloylated Graphene Oxide-Carbon Black Composite Polymer. *Biosens. Bioelectron.* **2019**, *135*, 36–44. [[CrossRef](#)] [[PubMed](#)]
97. Singh, R.; Singh, M. Highly Selective and Specific Monitoring of Pollutants Using Dual Template Imprinted MIP Sensor. *J. Electroanal. Chem.* **2022**, *926*, 116939. [[CrossRef](#)]
98. Thimoonnee, S.; Somnet, K.; Ngaosri, P.; Chairam, S.; Karuwan, C.; Kamsong, W.; Tuantranont, A.; Amatongchai, M. Fast, Sensitive and Selective Simultaneous Determination of Paraquat and Glyphosate Herbicides in Water Samples Using a Compact Electrochemical Sensor. *Anal. Methods* **2022**, *14*, 820–833. [[CrossRef](#)] [[PubMed](#)]
99. Núñez, O.; Moyano, E.; Puignou, L.; Galceran, M.T. Sample Stacking with Matrix Removal for the Determination of Paraquat, Diquat and Difenzoquat in Water by Capillary Electrophoresis. *J. Chromatogr. A* **2001**, *912*, 353–361. [[CrossRef](#)] [[PubMed](#)]
100. Guo, J.J.; Zhang, Y.; Luo, Y.L.; Shen, F.; Sun, C.Y. Efficient Fluorescence Resonance Energy Transfer Between Oppositely Charged CdTe Quantum Dots and Gold Nanoparticles for Turn-on Fluorescence Detection of Glyphosate. *Talanta* **2014**, *125*, 385–392. [[CrossRef](#)]
101. Rao, H.; Liu, X.; Ding, F.; Wan, Y.; Zhao, X.; Liang, R.; Zou, P.; Wang, Y.; Wang, X.; Zhao, Q. Nitrogen-doped Carbon Nanosheet Frameworks Decorated with Fe and Molecularly Imprinted Polymer for Simultaneous Detection of Mebendazole and Catechol. *Chem. Eng. J.* **2018**, *338*, 478–487. [[CrossRef](#)]
102. Ahmed, J.; Ahamad, T.; AlShehri, S.M. Iron-Nickel Nanoparticles as Bifunctional Catalysts in Water Electrolysis. *Chemelectrochem* **2017**, *4*, 1222–1226. [[CrossRef](#)]
103. Yang, C.; Denno, M.E.; Pyakurel, P.; Venton, B.J. Recent Trends in Carbon Nanomaterial-Based Electrochemical Sensors for Biomolecules: A Review. *Anal. Chim. Acta* **2015**, *887*, 17–37. [[CrossRef](#)] [[PubMed](#)]
104. Golabi, M.; Kuralay, F.; Jager, E.W.H.; Beni, V.; Turner, A.P.F. Electrochemical Bacterial Detection Using Poly(3-Aminophenylboronic Acid)-Based Imprinted Polymer. *Biosens. Bioelectron.* **2017**, *93*, 87–93. [[CrossRef](#)] [[PubMed](#)]
105. Tokonami, S.; Nakadoi, Y.; Takahashi, M.; Ikemizu, M.; Kadoma, T.; Saimatsu, K.; Dung, L.Q.; Shiigi, H.; Nagaoka, T. Label-Free and Selective Bacteria Detection Using a Film with Transferred Bacterial Configuration. *Anal. Chem.* **2013**, *85*, 4925–4929. [[CrossRef](#)] [[PubMed](#)]
106. Ayankojo, A.G.; Boroznjak, R.; Reut, J.; Öpik, A.; Syrinski, V. Molecularly Imprinted Polymer Based Electrochemical Sensor for Quantitative Detection of SARS-CoV-2 Spike Protein. *Sens. Actuators B-Chem.* **2022**, *353*, 131160. [[CrossRef](#)] [[PubMed](#)]
107. Tanchaoren, C.; Sukjee, W.; Thepparit, C.; Jaimipuk, T.; Auewarakul, P.; Thitithanyanont, A.; Sangma, C. Electrochemical Biosensor Based on Surface Imprinting for Zika Virus Detection in Serum. *ACS Sens.* **2019**, *4*, 69–75. [[CrossRef](#)] [[PubMed](#)]
108. Amorim, M.S.; Sales, M.G.F.; Frasco, M.F. Recent Advances in Virus Imprinted Polymers. *Biosens. Bioelectron. X* **2022**, *10*, 100131. [[CrossRef](#)]
109. Dar, K.K.; Shao, S.; Tan, T.; Lv, Y. Molecularly Imprinted Polymers for the Selective Recognition of Microorganisms. *Biotechnol. Adv.* **2020**, *45*, 107640. [[CrossRef](#)]
110. Crapnell, R.D.; Hudson, A.; Foster, C.W.; Eersels, K.; van Grinsven, B.; Cleij, T.J.; Banks, C.E.; Peeters, M. Recent Advances in Electrosynthesized Molecularly Imprinted Polymer Sensing Platforms for Bioanalyte Detection. *Sensors* **2019**, *19*, 1204. [[CrossRef](#)] [[PubMed](#)]
111. Chen, S.; Chen, X.; Zhang, L.; Gao, J.; Ma, Q. Electrochemiluminescence Detection of Escherichia coli O157: H7 Based on a Novel Polydopamine Surface Imprinted Polymer Biosensor. *ACS Appl. Mater. Interfaces* **2017**, *9*, 5430–5436. [[CrossRef](#)] [[PubMed](#)]
112. Yasmeen, N.; Etienne, M.; Sharma, P.S.; El-Kirat-Chatel, S.; Helú, M.B.; Kutner, W. Molecularly Imprinted Polymer As a Synthetic Receptor Mimic for Capacitive Impedimetric Selective Recognition of *Escherichia coli* K-12. *Anal. Chim. Acta* **2021**, *1188*, 339177. [[CrossRef](#)] [[PubMed](#)]
113. Shan, X.L.; Yamauchi, T.; Shiigi, H.; Nagaoka, T. Binding Constant of the Cell-shaped Cavity Formed on a Polymer for Escherichia Coli O157. *Anal. Sci.* **2018**, *34*, 483–486. [[CrossRef](#)] [[PubMed](#)]
114. Wu, J.K.; Wang, R.N.; Lu, Y.F.; Jia, M.; Yan, J.; Bian, X.J. Facile Preparation of a Bacteria Imprinted Artificial Receptor for Highly Selective Bacterial Recognition and Label-Free Impedimetric Detection. *Anal. Chem.* **2019**, *91*, 1027–1033. [[CrossRef](#)]
115. Bezdekova, J.; Hutarova, J.; Tomeckova, K.; Vaculovicova, M. Isolation and Detection of Bacteria Using Magnetic Molecularly Imprinted Polymers. In Proceedings of the 25th International Phd Students Conference (Mendelnet 2018), Brno, Czechia, 7–8 November 2018; pp. 484–488.
116. Yasmeen, N.; Etienne, M.; Sharma, P.S.; Kutner, W. Artificial Receptors for Electrochemical Sensing of Bacteria. *Curr. Opin. Electrochem.* **2023**, *39*, 101291. [[CrossRef](#)]
117. Roushani, M.; Sarabaegi, M.; Rostamzad, A. Novel Electrochemical Sensor Based on Polydopamine Molecularly Imprinted Polymer for Sensitive and Selective Detection of *Acinetobacter baumannii*. *J. Iran. Chem. Soc.* **2020**, *17*, 2407–2413. [[CrossRef](#)]
118. Buensuceso, C.E.; Tiu, B.D.B.; Lee, L.P.; Sabido, P.M.G.; Nuesca, G.M.; Caldon, E.B.; del Mundo, F.R.; Advincula, R.C. Electropolymerized-molecularly Imprinted Polymers (E-MIPS) As Sensing Elements for the Detection of Dengue Infection. *Anal. Bioanal. Chem.* **2022**, *414*, 1347–1357. [[CrossRef](#)]



119. Idil, N.; Mattiasson, B. Imprinting of Microorganisms for Biosensor Applications. *Sensors* **2017**, *17*, 708. [[CrossRef](#)]
120. Le, H.H.T.; Dalsgaard, A.; Andersen, P.S.; Nguyen, H.M.; Ta, Y.T.; Nguyen, T.T. Large-Scale *Staphylococcus aureus* Foodborne Disease Poisoning Outbreak among Primary School Children. *Microbiol. Res.* **2021**, *12*, 43–52. [[CrossRef](#)]
121. Samadpour, M.; Stewart, J.; Steingart, K.; Addy, C.; Louderback, J.; McGinn, M.; Ellington, J.; Newman, T. Laboratory Investigation of an *E. coli* O157:H7 Outbreak Associated with Swimming in Battle Ground Lake, Vancouver, Washington. *J. Environ. Health* **2002**, *64*, 16–20, 25, 26.
122. Osborn, B.; Hatfield, J.; Lanier, W.; Wagner, J.; Oakeson, K.; Casey, R.; Bullough, J.; Kache, P.; Miko, S.; Kunz, J.; et al. Shiga Toxin-Producing *Escherichia coli* O157:H7 Illness Outbreak Associated with Untreated, Pressurized, Municipal Irrigation Water—Utah, 2023. *MMWR Morb. Mortal. Wkly. Rep.* **2024**, *73*, 411–416. [[CrossRef](#)] [[PubMed](#)]
123. Xu, X.L.; Lin, X.H.; Wang, L.L.; Ma, Y.X.; Sun, T.; Bian, X.J. A Novel Dual Bacteria-Imprinted Polymer Sensor for Highly Selective and Rapid Detection of Pathogenic Bacteria. *Biosensors* **2023**, *13*, 868. [[CrossRef](#)] [[PubMed](#)]
124. Prasad, B.B.; Fatma, S. One MoNomer Doubly Imprinted Dendrimer Nanofilm Modified Pencil Graphite Electrode for Simultaneous Electrochemical Determination of Norepinephrine and Uric Acid. *Electrochim. Acta* **2017**, *232*, 474–483. [[CrossRef](#)]
125. Hu, C.; Huang, H.; Sun, H.; Yan, Y.; Xu, F.; Liao, J. Simultaneous Analysis of Catechol and Hydroquinone by Polymelamine/CNT with Dual-Template Molecular Imprinting Technology. *Polymer* **2022**, *242*, 124593. [[CrossRef](#)]
126. Lu, Z.; Du, X.; Sun, M.; Zhang, Y.; Li, Y.; Wang, X.; Wang, Y.; Du, H.; Yin, H.; Rao, H. Novel Dual-Template Molecular Imprinted Electrochemical Sensor for Simultaneous Detection of CA And TPH Based on Peanut Twin-Like NiFe<sub>2</sub>O<sub>4</sub>/CoFe<sub>2</sub>O<sub>4</sub>/NCDs Nanospheres: Fabrication, Application and DFT Theoretical Study. *Biosens. Bioelectron.* **2021**, *190*, 113408. [[CrossRef](#)] [[PubMed](#)]
127. Zheng, W.; Zhao, M.; Liu, W.; Yu, S.; Niu, L.; Li, G.; Li, H.; Liu, W. Electrochemical Sensor Based on Molecularly Imprinted Polymer/Reduced Graphene Oxide Composite for Simultaneous Determination of Uric Acid and Tyrosine. *J. Electroanal. Chem.* **2018**, *813*, 75–82. [[CrossRef](#)]
128. Karazan, Z.M.; Roushani, M. Electrochemical Sensor Based on Molecularly Imprinted Copolymer for Selective and Simultaneous Determination of Ascorbic Acid and Tyrosine. *Anal. Bioanal. Chem. Res.* **2023**, *10*, 269–278. [[CrossRef](#)]
129. Li, X.; Li, Y.; Yu, P.; Tong, Y.; Ye, B.-C. A High Sensitivity Electrochemical Sensor Based on a Dual-Template Molecularly Imprinted Polymer for Simultaneous Determination of Clenbuterol Hydrochloride and Ractopamine. *Analyst* **2021**, *146*, 6323–6332. [[CrossRef](#)] [[PubMed](#)]
130. Vahidifar, M.; Es'haghi, Z. Magnetic Nanoparticle-Reinforced Dual-Template Molecularly Imprinted Polymer for the Simultaneous Determination of Oxazepam and Diazepam Using an Electrochemical Approach. *J. Anal. Chem.* **2022**, *77*, 625–639. [[CrossRef](#)]
131. Hao, P.; Zhu, R.; Tao, Y.; Jiang, W.; Liu, X.; Tan, Y.; Wang, Y.; Wang, D. Dual-Analyte Sensing with a Molecularly Imprinted Polymer Based on Enhancement-Mode Organic Electrochemical Transistors. *ACS Appl. Mater. Interfaces* **2023**, *15*, 30567–30579. [[CrossRef](#)] [[PubMed](#)]
132. Wang, X.; Liu, Y.; Liu, J.; Qu, J.; Huang, J.; Tan, R.; Yu, Y.; Wu, J.; Yang, J.; Li, Y.; et al. A Bifunctional Electrochemical Sensor for Simultaneous Determination of Electroactive and Non-Electroactive Analytes: A Universal Yet Very Effective Platform Serving Therapeutic Drug Monitoring. *Biosens. Bioelectron.* **2022**, *208*, 114233. [[CrossRef](#)]
133. Rawool, C.R.; Srivastava, A.K. A Dual Template Imprinted Polymer Modified Electrochemical Sensor Based on Cu Metal Organic Framework/Mesoporous Carbon for Highly Sensitive and Selective Recognition of Rifampicin and Isoniazid. *Sens. Actuators. B Chem.* **2019**, *288*, 493–506. [[CrossRef](#)]
134. Li, N.; Nan, C.; Mei, X.; Sun, Y.; Feng, H.; Li, Y. Electrochemical Sensor Based on Dual-Template Molecularly Imprinted Polymer and Nanoporous Gold Leaf Modified Electrode for Simultaneous Determination of Dopamine and Uric Acid. *Mikrochim. Acta* **2020**, *187*, 496. [[CrossRef](#)] [[PubMed](#)]
135. Zhang, T.; Xuan, X.; Li, M.; Li, C.; Li, P.; Li, H. Molecularly Imprinted Ni-Polyacrylamide-Based Electrochemical Sensor for the Simultaneous Detection of Dopamine and Adenine. *Anal. Chim. Acta* **2022**, *1202*, 339689. [[CrossRef](#)]
136. Vahidifar, M.; Es'haghi, Z.; Oghaz, N.M.; Mohammadi, A.A.; Kazemi, M.S. Multi-template Molecularly Imprinted Polymer Hybrid Nanoparticles for Selective Analysis of Nonsteroidal Anti-Inflammatory Drugs and Analgesics in Biological and Pharmaceutical Samples. *Environ. Sci. Pollut. Res. Int.* **2022**, *29*, 47416–47435. [[CrossRef](#)]
137. Whitesides, G.M. The Origins and the Future of Microfluidics. *Nature* **2006**, *442*, 368–373. [[CrossRef](#)]
138. Regmi, S.; Poudel, C.; Adhikari, R.; Luo, K.Q. Applications of Microfluidics and Organ-on-a-Chip in Cancer Research. *Biosensors* **2022**, *12*, 459. [[CrossRef](#)] [[PubMed](#)]
139. Qi, J.; Li, B.W.; Zhou, N.; Wang, X.Y.; Deng, D.M.; Luo, L.Q.; Chen, L.X. The Strategy of Antibody-Free Biomarker Analysis by In-Situ Synthesized Molecularly Imprinted Polymers on Movable Valve Paper-Based Device. *Biosens. Bioelectron.* **2019**, *142*, 111533. [[CrossRef](#)] [[PubMed](#)]
140. Sharma, P.S.; Iskierko, Z.; Noworyta, K.; Cieplak, M.; Borowicz, P.; Lisowski, W.; D'Souza, F.; Kutner, W. Synthesis and Application of a “Plastic Antibody” in Electrochemical Microfluidic Platform for Oxytocin Determination. *Biosens. Bioelectron.* **2018**, *100*, 251–258. [[CrossRef](#)]



141. Kong, Q.K.; Wang, Y.H.; Zhang, L.N.; Xu, C.X.; Yu, J.H. Highly Sensitive Microfluidic Paper-based Photoelectrochemical Sensing Platform Based on Reversible Photo-Oxidation Products and Morphology Preferable Multi-plate ZnO Nanoflowers. *Biosens. Bioelectron.* **2018**, *110*, 58–64. [[CrossRef](#)] [[PubMed](#)]
142. Ge, L.; Wang, S.M.; Yu, J.H.; Li, N.Q.; Ge, S.G.; Yan, M. Molecularly Imprinted Polymer Grafted Porous Au-Paper Electrode for an Microfluidic Electro-Analytical Origami Device. *Adv. Funct. Mater.* **2013**, *23*, 3115–3123. [[CrossRef](#)]
143. Kellens, E.; Bove, H.; Vandenryt, T.; Lambrechts, J.; Dekens, J.; Drijkoningen, S.; D'Haen, J.; De Ceuninck, W.; Thoelen, R.; Junkers, T.; et al. Micro-patterned Molecularly Imprinted Polymer Structures on Functionalized Diamond-coated Substrates for Testosterone Detection. *Biosens. Bioelectron.* **2018**, *118*, 58–65. [[CrossRef](#)] [[PubMed](#)]
144. Liu, J.; Zhang, Y.; Jiang, M.; Tian, L.P.; Sun, S.G.; Zhao, N.; Zhao, F.L.; Li, Y.C. Electrochemical Microfluidic Chip Based on Molecular Imprinting Technique Applied for Therapeutic Drug Monitoring. *Biosens. Bioelectron.* **2017**, *91*, 714–720. [[CrossRef](#)]
145. Weng, C.H.; Yeh, W.M.; Ho, K.C.; Lee, G.B. A Microfluidic System Utilizing Molecularly Imprinted Polymer Films for Amperometric Detection of Morphine. *Sens. Actuators B-Chem.* **2007**, *121*, 576–582. [[CrossRef](#)]
146. Dincer, C.; Bruch, R.; Kling, A.; Dittrich, P.S.; Urban, G.A. Multiplexed Point-of-Care Testing—xPOCT. *Trends Biotechnol.* **2017**, *35*, 728–742. [[CrossRef](#)]
147. Fava, E.L.; Silva, T.A.; do Prado, T.M.; de Moraes, F.C.; Faria, R.C.; Fatibello, O. Electrochemical Paper-based Microfluidic Device for High Throughput Multiplexed Analysis. *Talanta* **2019**, *203*, 280–286. [[CrossRef](#)] [[PubMed](#)]
148. Somvanshi, S.B.; Ulloa, A.M.; Zhao, M.; Liang, Q.Y.; Barui, A.K.; Lucas, A.; Jadhav, K.M.; Allebach, J.P.; Stanciu, L.A. Microfluidic Paper-based Aptasensor Devices for Multiplexed Detection of Pathogenic Bacteria. *Biosens. Bioelectron.* **2022**, *207*, 114214. [[CrossRef](#)] [[PubMed](#)]
149. Glatz, R.T.; Ates, H.C.; Mohsenin, H.; Weber, W.; Dincer, C. Designing Electrochemical Microfluidic Multiplexed Biosensors for On-Site Applications. *Anal. Bioanal. Chem.* **2022**, *414*, 6531–6540. [[CrossRef](#)] [[PubMed](#)]
150. Volpetti, F.; Garcia-Cordero, J.; Maerkl, S.J. A Microfluidic Platform for High-Throughput Multiplexed Protein Quantitation. *PLoS ONE* **2015**, *10*, e0117744. [[CrossRef](#)] [[PubMed](#)]
151. Pérez-Alvarez, M.; Arroyo-Manzanares, N.; Campillo, N.; Viñas, P. Magnetic Molecularly Imprinted Polymers for Selective Extraction of Aflatoxins from Feeds. *Toxins* **2024**, *16*, 120. [[CrossRef](#)]
152. Orbay, S.; Sanyal, A. Molecularly Imprinted Polymeric Particles Created Using Droplet-Based Microfluidics: Preparation and Applications. *Micromachines* **2023**, *14*, 763. [[CrossRef](#)]
153. Lowdon, J.W.; Diliën, H.; Singla, P.; Peeters, M.; Cleij, T.J.; van Grinsven, B.; Eersels, K. MIPs for Commercial Application in Low-Cost Sensors and Assays—An Overview of the Current Status Quo. *Sens. Actuators B-Chem.* **2020**, *325*, 128973. [[CrossRef](#)]
154. Turner, N.W.; Jeans, C.W.; Brain, K.R.; Allender, C.J.; Hlady, V.; Britt, D.W. From 3D to 2D: A Review of the Molecular Imprinting of Proteins. *Biotechnol. Prog.* **2006**, *22*, 1474–1489. [[CrossRef](#)]
155. Dixit, C.K.; Bhakta, S.; Reza, K.K.; Kaushik, A. Exploring Molecularly Imprinted Polymers As Artificial Antibodies for Efficient Diagnostics and Commercialization: A Critical Overview. *Hybrid Adv.* **2022**, *1*, 100001. [[CrossRef](#)]
156. Baldoneschi, V.; Palladino, P.; Banchini, M.; Minunni, M.; Scarano, S. Norepinephrine as New Functional Monomer for Molecular Imprinting: An Applicative Study for the Optical Sensing of Cardiac Biomarkers. *Biosens. Bioelectron.* **2020**, *157*, 112161. [[CrossRef](#)]
157. Garcia-Mutio, D.; Gómez-Caballero, A.; Gotiandia, A.; Larrauri, I.; Goicolea, M.; Barrio, R. Controlled Grafting of Molecularly Imprinted Films on Gold Microelectrodes Using a Self-Assembled Thiol Iniferter. *Electrochim. Acta* **2018**, *279*, 57–65. [[CrossRef](#)]
158. Perez-Puyana, V.; Wieringa, P.; Guerrero, A.; Romero, A.; Moroni, L. (Macro)Molecular Imprinting of Proteins on PCL Electrospun Scaffolds. *ACS Appl. Mater. InterfacE* **2021**, *13*, 29293–29302. [[CrossRef](#)]
159. Ali, G.K.; Omer, K.M. Molecular Imprinted Polymer Combined with Aptamer (MIP-Aptamer) As a Hybrid Dual Recognition Element for Bio(Chemical) Sensing Applications. Review. *Talanta* **2022**, *236*, 122878. [[CrossRef](#)] [[PubMed](#)]
160. Liu, Y.X.; Dykstra, G. Recent Progress on Electrochemical (Bio)Sensors Based on Aptamer-Molecularly Imprinted Polymer Dual Recognition. *Sens. Actuators Rep.* **2022**, *4*, 100112. [[CrossRef](#)]
161. Phonklam, K.; Wannapob, R.; Sriwimol, W.; Thavarungkul, P.; Phairatana, T. A Novel Molecularly Imprinted Polymer PMB/MWCNTs Sensor for Highly-Sensitive Cardiac Troponin T Detection. *Sens. Actuators B-Chem.* **2020**, *308*, 127630. [[CrossRef](#)]
162. Rad, A.O.; Azadbakht, A. An Aptamer Embedded in a Molecularly Imprinted Polymer for Impedimetric Determination of Tetracycline. *Microchim. Acta* **2019**, *186*, 56. [[CrossRef](#)]
163. Mahmoud, A.M.; Alkahtani, S.A.; Alyami, B.A.; El-Wekil, M.M. Dual-recognition Molecularly Imprinted Aptasensor Based on Gold Nanoparticles Decorated Carboxylated Carbon Nanotubes for Highly Selective and Sensitive Determination of Histamine in Different Matrices. *Anal. Chim. Acta* **2020**, *1133*, 58–65. [[CrossRef](#)] [[PubMed](#)]
164. Li, S.H.; Ma, X.H.; Pang, C.H.; Tian, H.; Xu, Z.; Yang, Y.; Lv, D.Z.; Ge, H.L. Fluorometric Aptasensor for Cadmium(II) by Using an Aptamer-Imprinted Polymer As the Recognition Element. *Microchim. Acta* **2019**, *186*, 823. [[CrossRef](#)]
165. Shen, M.M.; Kan, X.W. Aptamer and Molecularly Imprinted Polymer: Synergistic Recognition and Sensing of Dopamine. *Electrochim. Acta* **2021**, *367*, 137433. [[CrossRef](#)]

166. Yuan, X.; Yuan, Y.; Gao, X.; Xiong, Z.; Zhao, L. Magnetic Dummy-template Molecularly Imprinted Polymers Based on Multi-Walled Carbon Nanotubes for Simultaneous Selective Extraction and Analysis of Phenoxy Carboxylic Acid Herbicides in Cereals. *Food Chem.* **2020**, *333*, 127540. [[CrossRef](#)] [[PubMed](#)]
167. Wang, X.; Luo, J.; Yi, C.; Liu, X. Paracetamol Sensor Based on Molecular Imprinting by Photosensitive Polymers. *Electroanalysis* **2013**, *25*, 1907–1916. [[CrossRef](#)]
168. Tadi, K.; Motghare, R.; Ganesh, V. Electrochemical Detection of Epinephrine Using a Biomimic Made Up of Hemin Modified Molecularly Imprinted Microspheres. *RSC Adv.* **2015**, *5*, 99115–99124. [[CrossRef](#)]
169. Abu-Alsoud, G.; Bottaro, C. Porous Thin-film Molecularly Imprinted Polymer Device for Simultaneous Determination of Phenol, Alkylphenol and Chlorophenol Compounds in Water. *Talanta* **2021**, *223*, 121727. [[CrossRef](#)] [[PubMed](#)]
170. Tamboli, V.; Bhalla, N.; Jolly, P.; Bowen, C.; Taylor, J.; Bowen, J.; Allender, C.; Estrela, P. Hybrid Synthetic Receptors on MOSFET Devices for Detection of Prostate Specific Antigen in Human Plasma. *Anal. Chem.* **2016**, *88*, 11486–11490. [[CrossRef](#)]
171. Agar, M.; Laabei, M.; Leese, H.S.; Estrela, P. Aptamer-Molecularly Imprinted Polymer Sensors for the Detection of Bacteria in Water. *Biosens. Bioelectron.* **2024**, *in press*. [[CrossRef](#)]
172. Gros, M.; Pizzolato, T.; Petrovic, M.; de Alda, M.; Barceló, D. Trace Level Determination of B-Blockers in Waste Waters by Highly Selective Molecularly Imprinted Polymers Extraction Followed by Liquid Chromatography-Quadrupole-Linear Ion Trap Mass Spectrometry. *J. Chromatogr. A* **2008**, *1189*, 374–384. [[CrossRef](#)] [[PubMed](#)]
173. Yang, H.; Zhou, W.; Guo, X.; Chen, F.; Zhao, H.; Lin, L.; Wang, X. Molecularly Imprinted Polymer As SPE Sorbent for Selective Extraction of Melamine in Dairy Products. *Talanta* **2009**, *80*, 821–825. [[CrossRef](#)]

**Disclaimer/Publisher’s Note:** The statements, opinions and data contained in all publications are solely those of the individual author(s) and contributor(s) and not of MDPI and/or the editor(s). MDPI and/or the editor(s) disclaim responsibility for any injury to people or property resulting from any ideas, methods, instructions or products referred to in the content.